DEVELOPMENTAL DYNAMICS 236:2258–2267, 2007

Development of Murine Hepatic Sinusoidal Endothelial Cells Characterized by the Expression of Hyaluronan Receptors

Hidenori Nonaka,[1,2] Minoru Tanaka,[1] Kaori Suzuki,[1] and Atsushi Miyajima[1,3]*

Endothelial cells (ECs) display distinct structural and functional characteristics depending on the tissue and developmental stage; however, the development of tissue-specific ECs remains poorly understood. Here, we describe the development of hepatic sinusoids in mice based on the expression of hyaluronan receptors Stab2 and Lyve-1. Flk-1$^+$ cells in and around the liver bud begin to express Stab2 at embryonic day (E) 9.5, before the formation of vascular lumen. Hepatic sinusoidal endothelial cells (HSECs) begin to express Lyve-1 at E10.5, and both markers continue to be expressed in HSECs thereafter. Although HSECs and lymphatic ECs (LECs) are known to share functional and phenotypic characteristics, we clearly show that HSECs can be distinguished from LECs by the expression of molecular markers and higher endocytotic activity. Our results provide new insight into the development of tissue-specific ECs and phenotypic criteria to distinguish HSECs from other types of ECs, including LECs. *Developmental Dynamics 236: 2258–2267, 2007.* © 2007 Wiley-Liss, Inc.

Key words: Flk-1; Stab2; Lyve-1; lymphatics; endocytotic activity

Accepted 8 May 2007

INTRODUCTION

Endothelial cells (ECs) are a heterogeneous cell population that displays distinct structural and functional characteristics depending on the tissue and developmental stage (Aird, 2003). Recently, several markers have been identified for some types of vascular cells: for example, lymphatic vessel endothelial hyaluronan receptor-1 (Lyve-1), podoplanin (Pdpn), and prospero-related homeobox 1 (Prox1) as lymphatic EC (LEC) markers (Oliver, 2004); ephrinB2 as an arterial EC marker; and EphB4 as a venous EC marker (Wang et al., 1998). These markers have contributed significantly to the understanding of EC development at the cellular and molecular levels (Carmeliet, 2003; Oliver, 2004). However, the development of tissue-specific microvascular ECs remains poorly understood (Cleaver and Melton, 2003) because of the lack of enough molecular markers to distinguish various types of microvascular ECs.

Hepatic sinusoidal endothelial cells (HSECs) line sinusoids to form an interface between the blood circulation and hepatocytes, and they are actively engaged in the clearance of various substances from the gut by means of their high endocytotic activity (Smedsrod et al., 1990; Braet and Wisse, 2002). Moreover, recent studies revealed that HSECs play an active role in liver development (Matsumoto et al., 2001), regeneration (LeCouter et al., 2003), and immune responses (Knolle and Limmer, 2003).

Immunophenotyping studies of human HSECs demonstrated that adult HSECs are characterized by the expression of the receptors II (CD32)

[1]Laboratory of Cell Growth and Differentiation, Institute of Molecular and Cellular Biosciences, The University of Tokyo, Bunkyo-ku, Tokyo, Japan
[2]Japan Health Sciences Foundation, Chuo-ku, Tokyo, Japan
[3]Core Research for Evolutional Science and Technology (CREST), Japan Science and Technology Agency, Kawaguchi, Saitama, Japan
Grant sponsor: Ministry of Education, Culture, Sports, Science and Technology; Grant sponsor: CREST program of Japan Science and Technology; Grant sponsor: Ministry of Health, Labour and Welfare, Japan.
***Correspondence to: Atsushi Miyajima, PhD, Laboratory of Cell Growth and Differentiation, Institute of Molecular and Cellular Biosciences, The University of Tokyo, 1-1-1 Yayoi, Bunkyo-ku, Tokyo 113-0032, Japan.**
E-mail: miyajima@iam.u-tokyo.ac.jp

DOI 10.1002/dvdy.21227
Published online 11 July 2007 in Wiley InterScience (www.interscience.wiley.com).

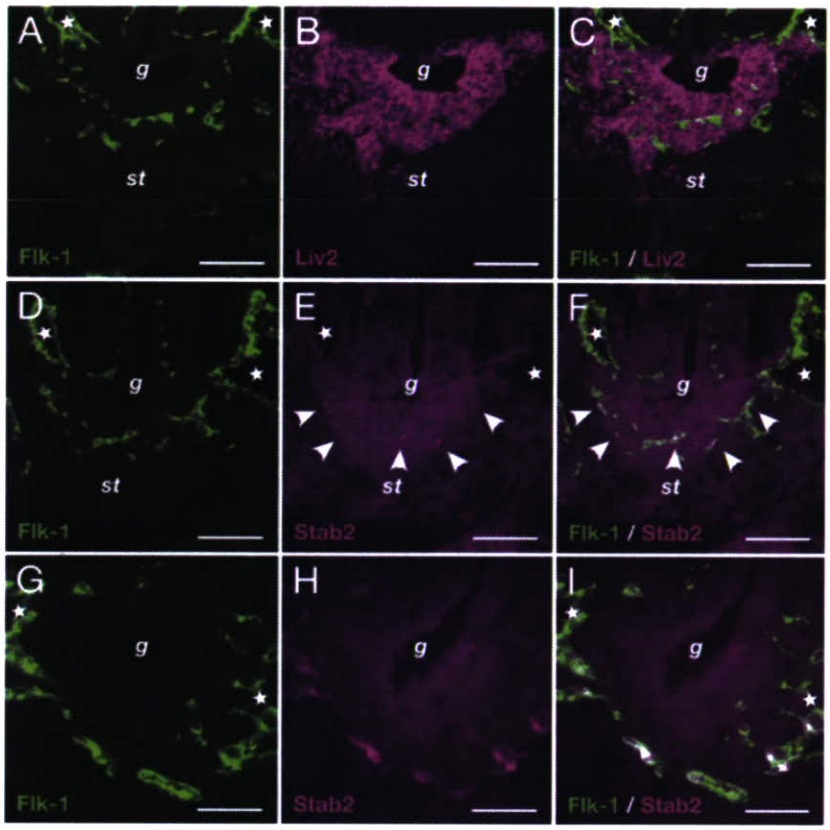

Fig. 1. Emergence of Flk-1$^+$Stab2$^+$ cells in the developing liver bud. **A–I:** Double staining of transverse sections of embryonic day (E) 9.5 mouse embryos (20–25 somite stages) with antibodies against Flk-1 and Liv2 (green and magenta, respectively, in A–C) or Flk-1 and Stab2 (green and magenta, respectively, in D–I) as indicated. C,F,I: Merged images of A,B, D,E, and G,H, respectively. The section in D–F is the most proximal to that in A–C. The section in G–I is from the caudal part of the foregut. A fraction of the Flk-1$^+$ cells in the liver bud also express Stab2 (arrowhead in D–F, white signals in F). In the caudal part of the foregut, the expression of Liv2 was not detected (data not shown) but Flk-1$^+$ cells also expressed Stab2 (G–I, white signals in I). All images are representative of at least three independent samples. st, septum transversum; g, foregut; asterisks, vitelline vein. Scale bars = 80 μm in A–F, 40 μm in G–I.

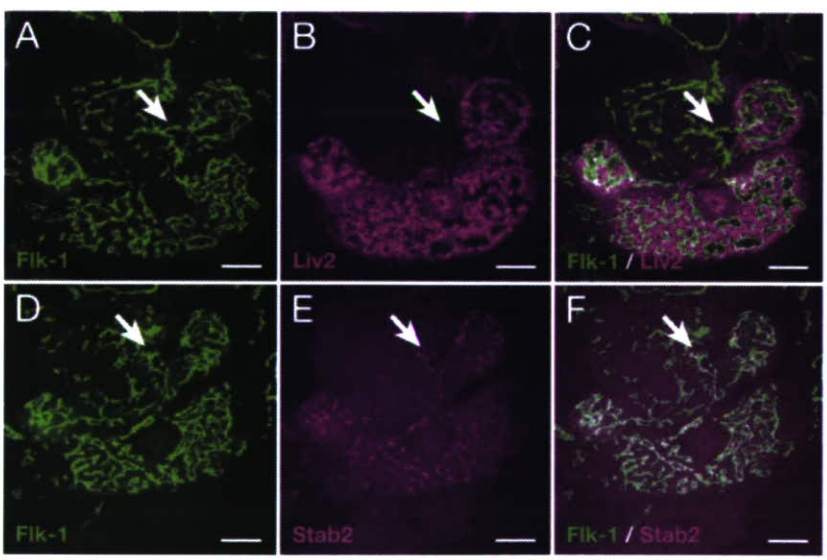

Fig. 2.

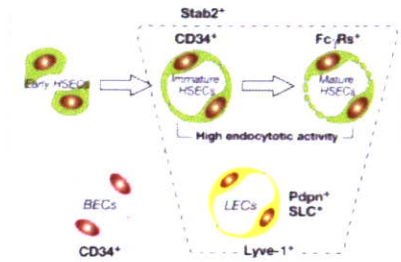

Fig. 6. A schematic diagram of the endothelial cells (EC) profiles. Based on our results presented here, each EC is recognizable by expression of the genes indicated. Endocytotic activity also distinguishes different types of ECs.

and III (CD16) for the Fc fragment of IgG (FcγRs) but lack sialomucin CD34, a marker for continuous microvascular ECs (Scoazec and Feldmann, 1991). In humans, these characteristics become evident at the mid-stage of liver development (Couvelard et al., 1996). Likewise, in rats, HSEC specification becomes evident as indicated by the expression of the SE-1 antigen at the mid-stage of liver development (Morita et al., 1998). In mice, fenestrated linings, one of the typical features of hepatic sinusoids, are observed at embryonic day 15 (E15), although they are incomplete at this stage (Enzan et al., 1997). These observations indicate that HSEC specification is evident at the mid-stage of liver development in mammals. However, it remains unknown when ECs acquire the distinct phenotype during liver development and the differences between adult mature HSECs and fetal immature HSECs remain obscure.

HSEC markers with scavenger functions have recently been described. Stabilin-2 (Stab2) is a fasciclin domain-containing hyaluronan receptor that binds to a variety of mol-

Fig. 2. Expression of Stab2 in extrahepatic vein. **A–F:** Double staining of transverse sections of embryonic day (E) 9.75 mouse embryos (around the 35 somite stage) with antibodies against Flk-1 and Liv2 (green and magenta, respectively, in A–C) or Flk-1 and Stab2 (green and magenta, respectively, in D–F) as indicated. C,F: Merged images of A,B and D,E, respectively. The section in D–F is proximal to that in A–C. Almost all of the Flk-1$^+$ ECs in the liver express Stab2. Endothelial cells (ECs) of the extrahepatic vitelline veins (arrow) also express Stab2. All images are representative of at least three independent samples. Scale bars = 100 μm in A–F.

ecules (Politz et al., 2002; Adachi and Tsujimoto, 2002; Hansen et al., 2005). Stab2 is constitutively expressed in adult HSECs, and its expression is restricted to the sinusoidal endothelia in vasculature, namely to the liver, lymph nodes, spleen, and bone marrow (Zhou et al., 2000; Falkowski et al., 2003; Nonaka et al., 2004). Lyve-1 is also an endocytotic receptor for hyaluronan and is predominantly expressed in LECs (Banerji et al., 1999). Lyve-1 expression is also observed in both fetal and adult HSECs (Carreira et al., 2001; Morisada et al., 2005).

Because the expression of Stab2 and Lyve-1 is restricted to specific types of ECs, they could be markers to monitor the process of the differentiation of tissue-specific ECs from pre-existing ECs or endothelial progenitors. In this study, we immunohistochemically examined the expression of these receptors together with other endothelial markers in mice. We showed that ECs in and around the liver bud acquire the distinct phenotype at E9.5. Furthermore, we clearly defined the phenotypes of fetal (E14.5) immature and adult mature HSECs by flow cytometry, reverse transcriptase-polymerase chain reaction (RT-PCR) and in vitro functional analysis. Our results provide new insight into the development of tissue-specific ECs and phenotypic criteria to distinguish HSECs from other types of ECs, including LECs. The results also demonstrate that the liver provides a unique model for studies on EC development.

RESULTS

Emergence of Flk-1$^+$Stab2$^+$ Cells in the Developing Liver Bud

In mammals, HSEC specification is evident at the mid-stage of liver development (i.e., 10 weeks of gestation in humans, E15 in rats, and E15 in mice) as indicated by gene expression profiles and fenestrae formation. However, it is unknown when ECs acquire the distinct phenotype of HSECs during liver development. To address this issue and to clarify the developmental processes that produce liver sinusoids, we used new markers for HSECs, Stab2 and Lyve-1, and immunohistochemically examined the expression of these receptors together with Flk-1 (an endothelial marker) and Liv2 (a hepatoblast marker; Watanabe et al., 2002) in mice.

It is known that, at E9.5 (20–25 somite stages), hepatoblasts emerge from the foregut endoderm and invade into the mesenchyme of the septum transversum (STM). These hepatoblasts were recognized by the Liv2 antibody (Fig. 1B). Flk-1$^+$ cells (ECs or EC progenitors) were observed in the vitelline veins (Fig. 1, asterisks), foregut, and liver bud (Fig. 1A,C). It should be noted that Flk1$^+$ cells in the foregut and liver bud did not form the vascular lumen. In the same region, a fraction of the Flk-1$^+$ cells coexpressed Stab2 (arrowhead in Fig. 1D–F, this section is the most proximal to those shown in Fig. 1A–C). In contrast, Lyve-1 expression was not detected at this stage (data not shown). In the caudal part of the foregut, endodermal cells did not invade the surrounding mesenchyme (Fig. 1G–I) and Liv2 was not expressed (data not shown). In this region, Flk-1$^+$ cells were observed in the vitelline veins and also around the Liv2$^-$ foregut (Fig. 1G,I). Of interest, these Flk-1$^+$ cells also expressed Stab2 (Fig. 1G–I). Stab2 expression was not detected in other regions of the embryo proper, such as head, heart, and tail (data not shown). These results indicated that, at E9.5, Flk1$^+$ cells in the liver bud and around the foregut were distinct from the ones in other regions. It should be noted that Flk-1$^+$Stab2$^+$ cells appeared before the formation of the vascular lumen.

Stab2 Expression in the Extrahepatic Veins and Intrahepatic Large Vessels

We further analyzed the expression of the markers during the course of liver development. At E9.75 (approximately the 35 somite stage), the liver became enlarged, lobe structures were recognizable, and Flk-1$^+$ ECs formed primitive vascular lumen (Fig. 2A–C). As shown in Figure 2D–F, almost all of the Flk-1$^+$ cells expressed Stab2. The Stab2 signals were stronger at E9.75 than at E9.5 (Figs. 1, 2). Moreover, Stab2 expression was also detected in the vitelline veins (arrow in Fig. 2), which was close to but not within the liver lobes (Liv2$^+$ region in Fig. 2A–C). On the other hand, Stab2 expression was hardly detectable in the gut ECs (upper region of the liver in Fig. 2). These results indicated that both HSECs and vitelline vein ECs share a common feature, which differs from that of the other ECs.

The vitelline and umbilical veins drain into the liver at E10.5 (arrows in Fig. 3A–D), and they will form the portal veins and the ductus venosus later (Kaufman, 1995). At E10.5, Stab2 expression was detected in both sinusoids and large vessels (vitelline and umbilical veins) in the liver (Fig. 3A,C) where Liv2 was expressed (Fig. 3B). Lyve-1 expression could also be detected in part of sinusoids and large vessels (Fig. 3D). These results suggested that large vessels draining into the liver continued to express Stab2, and a part of the Stab2$^+$ HSECs became Lyve-1$^+$ at this stage. Expression of Stab2 and Lyve-1 in large vessels was observed during the subsequent stages of embryonic liver development (immunohistochemical images of E14.5 and E17.5 liver are shown in Fig. 3E,F and G,H, respectively). These results indicate that ECs in the portal and the central veins share a common feature during the fetal period. As the liver development proceeds, portal triads are formed, and the hepatic artery and lymphatic vessels are observed around the portal veins (data not shown). The expression of Stab2 in ECs in the large vessels decreased after birth (data not shown). It appears that both Stab2 and Lyve-1 are continuously expressed in HSECs throughout liver development, whereas both receptors are transiently expressed in the other ECs in the liver during the fetal period.

Characterization of Fetal and Adult HSECs

To define HSECs in detail and to reveal the differences between fetal immature (at E14.5) and adult mature HSECs, we compared the expression of surface markers by flow cytometry. Simultaneously, we also compared HSECs with other types of ECs, in particular LECs. Although HSECs and LECs are known to share some

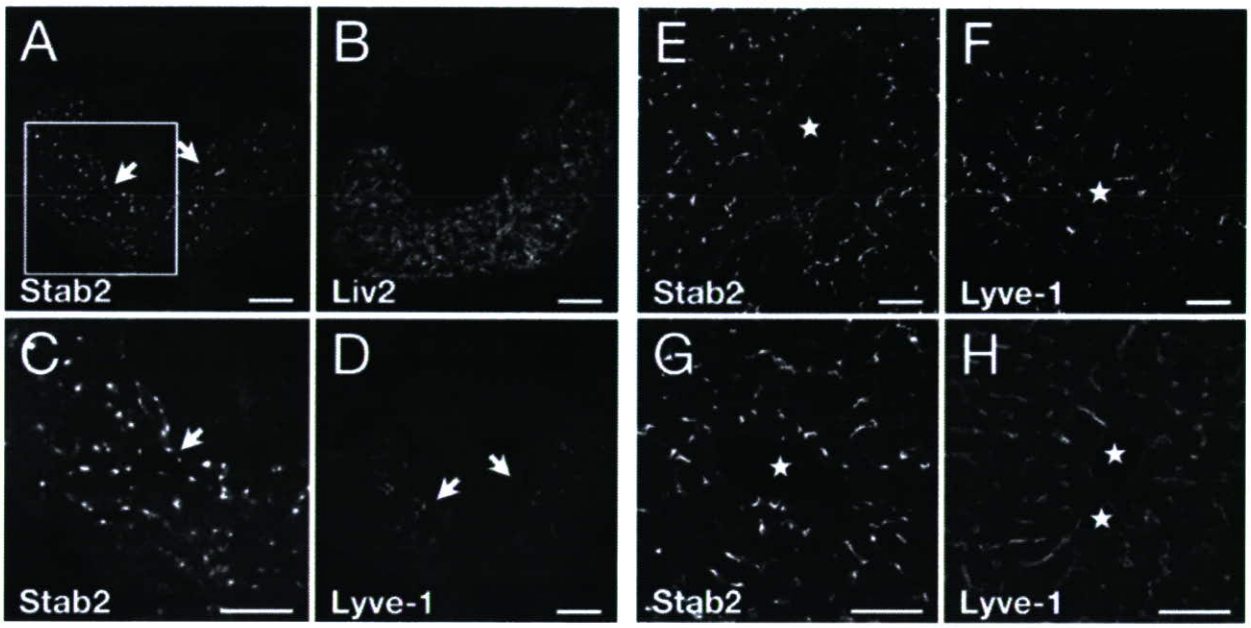

Fig. 3. Expression of Stab2 in intrahepatic large vessels. **A–H:** Staining of sections of embryonic day (E) 10.5 (A–D), E14.5 (E,F), and E17.5 (G,H) livers of mouse embryos with antibodies against Stab2 (A,C,E,G), Liv2 (B) and Lyve-1 (D,F,H) as indicated. C: Higher magnification of A (box). Expression of both Stab2 and Lyve-1 was detected in intrahepatic large vessels (arrows in A, C, D and asterisks in E–H). All images are representative of at least three independent samples. Scale bars = 100 μm in A,B,D–F, 80 μm in C,G,H.

functional and phenotypic characteristics (Lalor et al., 2006), such as Lyve-1 expression, the difference between HSECs and LECs is poorly understood.

E14.5 and adult liver cells contain various types of cells, including hepatocytes, ECs, Kupffer cells, stellate cells, blood cells, and so on. Based on cell density, adult hepatic cells can be divided into two fractions, parenchymal hepatocytes and others (nonparenchymal cells, NPCs), by low-speed centrifugation (Seglen, 1976). We prepared NPCs to analyze adult HSECs. EC fractions were recognized as $CD45^-CD31^+$ cells (boxes in Fig. 4A). Stab2 was expressed in 87% and 76% of $CD45^-CD31^+$ cells in E14.5 liver and adult liver NPCs, respectively (Fig. 4B). Lyve-1 was expressed in 95% and 79% of them (Fig. 4C). These results indicate that the major populations of $CD45^-CD31^+$ cells in the E14.5 liver and adult liver NPCs are $Stab2^+Lyve\text{-}1^+$ HSECs. Pdpn (another marker for LECs) expression was not detected in either fetal or adult HSECs, indicating that these HSECs are distinguishable from LECs according to their Pdpn expression (Fig. 4D). CD34 expression was detected in fetal but not adult HSECs (Fig. 4E). In contrast, FcγRs were detected only in adult but not fetal HSECs (Fig. 4F).

Cells from the E14.5 body (not including the liver) and adult lung were expected to contain both blood vascular ECs (BECs) and LECs. Indeed, a fraction of $CD45^-CD31^+$ cells from them were $Lyve\text{-}1^+$, representing LECs (Fig. 4C). In these cells, little or no expression of Stab2 was observed (Fig. 4B). $Stab2^+$ cells of lung ECs seemed to be derived from pulmonary lymph nodes. On the other hand, Pdpn expression was observed in a part of $CD45^-CD31^+$ cells, and all fetal as well as adult ECs expressed CD34 but not FcγRs (Fig. 4D–F). Taken together, these results indicate that a combination of these markers is able to distinguish HSECs at different developmental stages and also to distinguish HSECs from the other types of ECs (Fig. 6).

To further characterize HSECs, we performed RT-PCR analysis (Fig. 5A). By using a cell sorter, fetal HSECs were isolated from the E14.5 liver as $CD45^-CD31^+Lyve\text{-}1^+$ cells, and fetal BECs and LECs were isolated from the E14.5 body as $CD45^-CD31^+Lyve\text{-}1^-$ cells and $CD45^-CD31^+Lyve\text{-}1^+$ cells, respectively (Morisada et al., 2005). Adult HSECs were isolated from NPCs as $CD45^-Stab2^+$ cells, and adult BECs and LECs were isolated from the lung as $CD45^-CD31^+Pdpn^-$ cells and $CD45^-CD31^+Pdpn^+$ cells, respectively. All of these ECs expressed EC markers, CD31, VE-Cad and VWF, confirming the EC nature of the isolated cells. In accord with the results of flow cytometry, Stab2, Lyve-1, and FcγR2b, but not Pdpn, were detected in HSECs. Furthermore, secondary lymphoid chemokine (SLC), a LEC marker, was not detected in HSECs, and coagulation factor VIII (F8), an HSEC marker, was detected only in HSECs. Flt4, which is preferentially expressed in LECs, was also detected in HSECs, suggesting that vascular endothelial growth factor-C could act on HSECs. It should be noted that fetal and adult HSECs exhibited similar expression profiles by RT-PCR analysis; however, the expression levels of FcγRs and CD34 proteins were quite different between fetal and adult HSECs (Figs. 4, 5A).

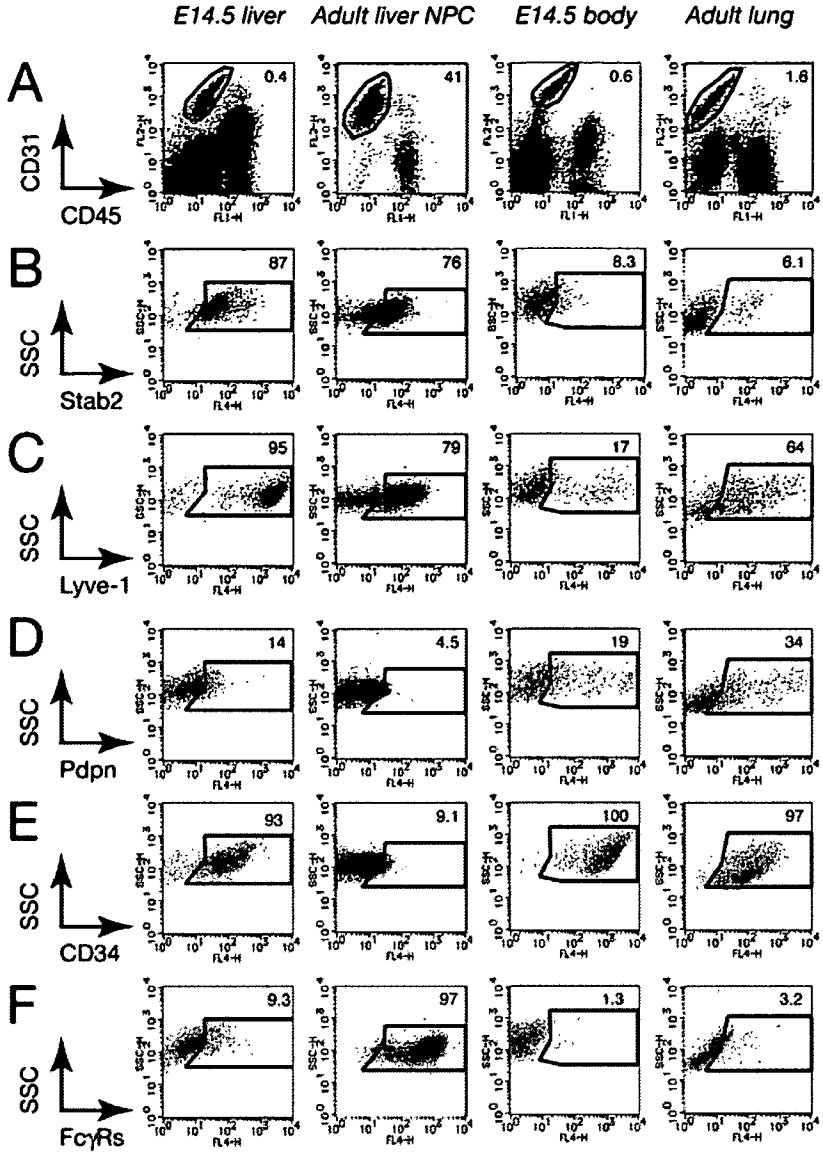

Fig. 4. Phenotypic characterization of $CD45^-CD31^-$ endothelial cells (ECs) from the liver and other tissues by flow cytometry. Cells obtained from each tissue were used as sources of material for flow cytometry. Cells were costained with antibodies against CD45, CD31 and the indicated proteins. **A:** EC gates were set on the CD45 vs. CD31 dot plots to contain $CD45^-CD31^+$ cells (boxes). **B–F:** The events in EC gates were then displayed on the side scatter vs. indicated proteins' dot plots. The numbers indicate percentages of cells in each box. All data are representative of at least three independent experiments.

Functional Difference Between HSECs and Other ECs From E14.5 Embryos

To analyze the functional differences among isolated ECs, their endocytotic activity was evaluated quantitatively by incorporation of acetylated low density lipoprotein labeled with 1,1′ -dioctadecyl -3,3,3′,3′ -tetramethylindo-carbocyanine perchlorate (DiI-Ac-LDL) in vitro (Fig. 5C). Simultaneously, Stab2 expression in cultured HSECs was examined by immunocytochemistry. As shown in Figure 5B, all of the isolated ECs were able to take up DiI-Ac-LDL, while only HSECs expressed Stab2. Interestingly, fetal HSECs exhibited higher endocytotic activity than the other ECs examined (Fig. 5C), indicating that they are functionally distinguishable from the other types of ECs.

DISCUSSION

The definition of tissue-specific ECs is needed for a precise understanding of their mechanisms of development. In this study, we characterized the fetal immature and adult mature HSECs in mice. At E9.5, $Flk\text{-}1^+$ cells in and around the liver bud begin to express Stab2, indicating that ECs acquire the distinct phenotype at this stage. One day after the Stab2 expression (E10.5), HSECs begin to express Lyve-1 and continue to express both markers thereafter. During the mid-fetal period (from E9.5 to E14.5), immature HSECs express CD34 but not FcγRs. Moreover, they do not form fenestrae (unpublished observation; Enzan et al., 1997). During the late fetal period (from E15.5 to birth), they begin to express other HSEC markers, such as FcγRs (unpublished observation), and the fenestrae become evident (Enzan et al., 1997), while CD34 is decreased. These observations suggest that HSEC differentiation is a multistep process. We detected at least three types of HSECs during liver development: (1) the early HSECs, $Flk\text{-}1^+Stab2^+$; (2) fetal immature HSECs, $Flk\text{-}1^+Stab2^+Lyve\text{-}1^+CD34^+$ $Fc\gamma Rs^-$fenestrae$^-$; and (3) adult mature HSECs, $Flk\text{-}1^+Stab2^+Lyve\text{-}1^+CD34^-Fc\gamma Rs^+$fenestrae$^+$ (Fig. 6). It should be noted that ECs in portal vein and central veins share common characteristics with HSECs during the fetal period, that is, expression of Stab2 and Lyve-1. However, they exhibit different characteristics after birth.

At E8.5 in mice, the cardiac mesoderm induces hepatic cell differentiation in the ventral endoderm (Gualdi et al., 1996). At E9.5, the specified hepatic cells migrate into the surrounding STM and form the liver bud. At the same time, $Flk\text{-}1^+$ ECs within and around the bud promote hepatic cell growth, morphogenesis, and differentiation (Matsumoto et al., 2001; Lammert et al., 2003). It is an intriguing question whether or not only $Stab2^+$ ECs, but not $Stab2^-$ ECs, induce the growth and differentiation of surrounding hepatic progenitors. Vascular development consists of two different processes: vasculogenesis and

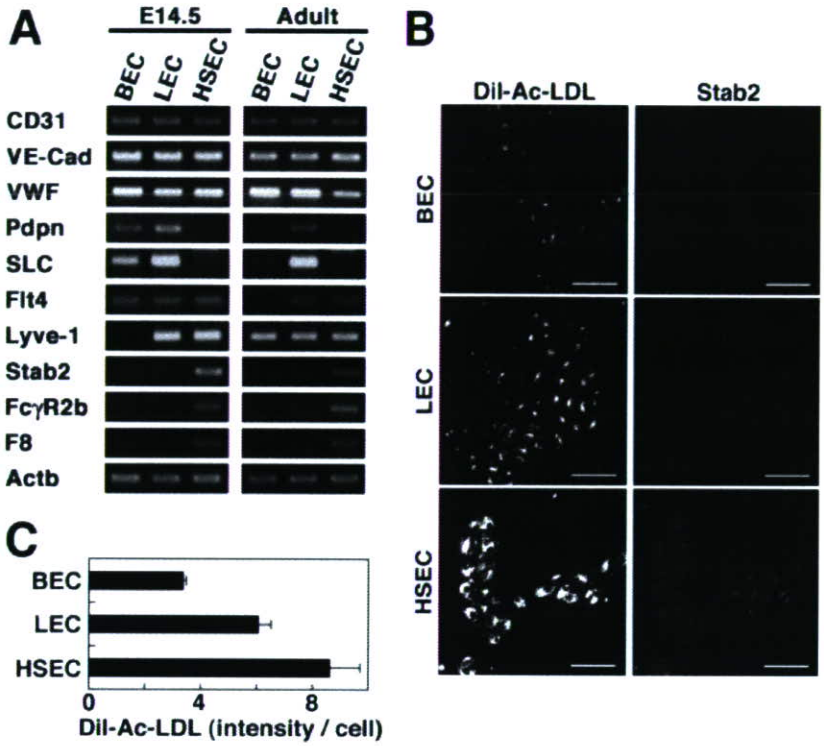

Fig. 5. Phenotypic characterization of Stab2$^+$ hepatic sinusoidal endothelial cells (HSECs). **A:** Polymerase chain reaction (PCR) analyses of genes that served as markers for endothelial cells (ECs), lymphatic ECs (LECs), and HSECs. Cells were isolated using a cell sorter. E14.5 blood vascular ECs (BECs), LECs, and HSECs were from the E14.5 embryos, adult BECs and LECs were from the lung, and adult HSECs were from adult liver nonparenchymal cells (NPCs). Total RNA was isolated and subjected to reverse transcriptase-PCR analyses. Neither podoplanin (Pdpn) nor secondary lymphoid chemokine (SLC) expression could be detected in HSECs. Little or no expression of FcγR2b, Stab2, or F8 was observed in BECs and LECs. All data are representative of at least three independent experiments. **B,C:** Endocytotic activity in cultured fetal mouse ECs was estimated by measuring cellular uptake of Dil-Ac-LDL. E14.5 BECs, LECs, and HSECs were isolated and cultured on fibronectin-coated dishes for 1 day and then incubated with 5 μg/ml of Dil-Ac-LDL at 37°C for 3 hr. Cells were fixed with 4% paraformaldehyde, stained with the antibody against Stab2 and then observed by fluorescence microscopy. Photomicrographs were taken (B) and the Dil fluorescence intensity was measured using AquaCosmos software (C). Results are expressed as the means ± SD from five different microscopic fields and are representative of three independent experiments. Scale bars = 80 μm in B.

angiogenesis. The HSEC phenotype appears before Flk-1$^+$ cells form the vascular lumen, suggesting that ECs acquire the distinct phenotype during vasculogenesis. We also observed that the Flk-1$^+$ cells protruding from the vitelline veins expressed Stab2, suggesting that HSECs also differentiate during angiogenesis.

The adult liver is a metabolic center of the body. In contrast, the embryonic liver has much less metabolic activity, and instead functions as a hematopoietic microenvironment (Orkin, 1996). Sinusoidal endothelial cells are found in hematopoietic organs, such as the liver, spleen, and bone marrow, and are known to express Stab2 (Falkowski et al., 2003). In the murine system, coincidentally with the emergence of Stab2$^+$ cells in the liver bud, fetal liver hematopoiesis begins at E10 (Sasaki and Sonoda, 2000). Of interest, before the emergence of Stab2$^+$ cells in the embryo proper, Stab2$^+$ ECs were observed in the yolk sac (unpublished observations) where primitive hematopoiesis occurs. Moreover, Stab2$^+$ cells were also found in the aorta–gonad–mesonephros region at E11.5 (unpublished observations) where definitive hematopoiesis starts. These observations suggest a possible involvement of Stab2 in hematopoiesis, for example, cell–cell adhesion or hematopoietic cell transmigration. This idea is supported by the fact that stabilin-1 (Stab1), a homolog of Stab2 and a member of the family of fasciclin domain-containing hyaluronan receptors (Adachi and Tsujimoto, 2002; Politz et al., 2002), mediates lymphocyte transmigration through vascular and lymphatic endothelium (Irjala et al., 2003; Salmi et al., 2004).

Lyve-1 was originally identified as a lymph-specific receptor for hyaluronan (Banerji et al., 1999), and a subsequent study revealed that its expression is not restricted to the lymph vessels but is also detected in normal adult HSECs (Carreira et al., 2001). In addition to Lyve-1 expression, HSECs are known to share other functional and phenotypic characteristics with LECs (e.g., minimal basement membranes, loose cell–cell adhesion, expression of VSP-1 (Bonder et al., 2005) and Reelin (Ikeda and Terashima, 1997; Samama and Boehm, 2005), and lack of CD34 (Lalor et al., 2006)). However, we show here that HSECs are clearly distinguishable from LECs. Stab2, FcγRs, and F8 are expressed in HSECs, but not in LECs. In contrast, Pdpn, SLC, and Prox1 are expressed in LECs, but not in HSECs (Fig. 6).

Another interesting feature of HSECs is their developmental origin. It is considered that portal veins are derived from vitelline veins and the sinusoids develop from the capillary vessels of the STM (Gouysse et al., 2002). In this study, we clearly showed that a part of the Flk-1$^+$ cells in both vitelline veins and the STM expressed Stab2, suggesting the possibility that HSECs are derived from both veins and mesenchyme. In the case of LECs, the earliest signs of LEC development are observed in the anterior cardinal veins and the vitelline veins (Wigle et al., 2002). Moreover, recent studies provide evidence for the existence of mesenchymal lymphangioblasts in the dermis, the mediastinum and the primitive meninx (Buttler et al., 2006). Although much remains to be learned about the HSEC development, there seems to be an intimate relationship between HSECs and LECs.

Although various differences in the cell surface phenotype among ECs have become clearer, the functional divergence is still not well docu-

mented. By using various markers, it has become possible to distinguish and to isolate different types of ECs. Our analysis of the uptake of DiI-Ac-LDL by BECs, LECs, and HSECs derived from E14.5 embryo revealed that fetal HSECs have already acquired high endocytotic activity (Fig. 5). This finding is the first evidence that HSECs in the E14.5 liver could be distinguished from the other types of ECs not only by marker gene expression but also by a functional indicator, namely endocytotic capacity. These results are consistent with the fact that, in mammals, elimination of hyaluronan from plasma takes place mainly in the liver not only in adult but also during fetal period (Fraser et al., 1985, 1989). The next important question is what signals control HSEC differentiation and maturation. Further analysis of several types of ECs will provide clues about the mechanisms of HSEC development. As the liver contains various types of ECs, it provides a novel system to study the development of the vascular system and the roles of ECs in organogenesis.

EXPERIMENTAL PROCEDURES

Animals

C57BL/6J mice (Nihon Clea, Tokyo, Japan) were used for the immunohistochemical experiments. The age of the embryos was determined by days after appearance of the vaginal plug. Noon of this day was considered as E0.5. All procedures were approved by the institutional animal care and use committee of the University of Tokyo.

Development of Monoclonal Antibodies

To generate a monoclonal antibody (mAb) against the extracellular part of Stab2, a 4062-bp fragment of mouse Stab2 cDNA (positions 3491-7552 in GenBank clone NM_138673.1) was amplified by PCR and was inserted into the mammalian expression vector pME18S (Takebe et al., 1988). BaF3 cells were transfected with the expression vector, and cells stably expressing Stab2 were used for the immunization. The lymph node cells isolated from an immunized rat were fused with mouse myeloma P3X cells. Hybridomas were screened for staining activity of a stable line of NIH3T3 cells transfected with Stab2. As a result, we established four hybridoma clones. These mAbs could be used for flow cytometry and also for immunohistochemistry on frozen sections.

Anti-mouse Lyve-1 mAb was obtained by immunizing a rat with mouse fetal hepatic cells. Fetal hepatic cells were isolated from E14.5 mouse embryos (Kamiya et al., 1999), and $CD45^-/TER119^-$ cells were isolated using an automatic magnetic cell sorter (AutoMACS; Miltenyi Biotec GmbH, Bergisch Gladbach, Germany; Tanimizu et al., 2003) and used for the immunization. The supernatants of hybridoma cells were used for an immunohistochemical screening assay against E14.5 and adult liver. One of the hybridoma clones, 14-4, produced a mAb against fetal sinusoids and adult hepatic lymphatics. To identify the 14-4 antigen, retrovirus-mediated expression cloning was performed (Kitamura et al., 1995). To confirm the reactivity of 14-4 mAb with mouse Lyve-1, Lyve-1-transfected or mock-transfected BaF3 cells (kindly provided by Dr. Y. Oike; Morisada et al., 2005) were stained with the mAb, and analyzed with a FACSCalibur flow cytometer (BD Biosciences, San Jose, CA).

Antibodies

The primary antibodies used were rat anti-mouse Stab2 mAb, rat anti-mouse Lyve-1 (generated in our laboratory as mentioned above); goat anti-mouse vascular endothelial growth factor receptor-2 (Flk-1) polyclonal antibody (R&D Systems, Minneapolis, MN); rat anti-Liv2 mAb (Watanabe et al., 2002; kindly provided by Dr. H. Nishina); rat anti-mouse Pdpn mAb (Watanabe et al., 1988; Kato et al., 2004; kindly provided by Drs. N. Fujita and T. Tsuruo); anti-mouse CD16/32 mAb, fluorescein isothiocyanate (FITC) -conjugated anti-mouse CD16/32 mAb, FITC-conjugated anti-mouse CD45 mAb, phycoerythrin (PE) -conjugated anti-mouse CD31 mAb, and biotinylated anti-mouse CD34 mAb (BD Biosciences Pharmingen, San Diego, CA). Antibodies against Stab2, Lyve-1 (14-4), and Pdpn were labeled with biotin using the Amersham ECL Protein Biotinylation Module (GE Healthcare UK Ltd., Buckinghamshire, England). The secondary antibodies and reagents used were FITC-conjugated rabbit anti-goat IgG (Pierce Biotechnology, Rockford, IL); rhodamine-conjugated chicken anti-rat IgG (Santa Cruz Biotechnology, Inc., Santa Cruz, CA); PE-conjugated anti-rat IgG (BD Biosciences Pharmingen); biotinylated rabbit anti-rat IgG (Vector Laboratories, Burlingame, CA); and allophycocyanin (APC) -conjugated streptavidin (Invitrogen Corp., Carlsbad, CA).

Immunostaining

Embryos and livers were embedded in OCT compound (Sakura Finetek Japan Co., Ltd., Tokyo, Japan). Eight-micrometer sections were prepared with a Microm HM505E cryostat (MICROM International GmbH, Waldorf, Germany) and mounted on glass slides coated with APS (Matsunami glass Ind. Ltd., Osaka, Japan). They were fixed with 4% paraformaldehyde (PFA) in phosphate buffered saline (PBS) for 15 min. For immunohistological staining, sections were treated with 0.3% H_2O_2 in PBS, incubated with 2% skim milk in PBS, and incubated with the primary antibodies followed by incubation with the biotin-conjugated secondary antibody. The signals were detected using a Vectastatin ABC kit (Vector) and 3,3-diaminobenzidine tetrahydrochloride. Images were captured using an Axioskop2 plus microscope (Carl Zeiss, Oberkochen, Germany) with a DXM1200 digital camera (Nikon, Tokyo, Japan) and an ACT-1 software (Nikon). For immunofluorescence staining, sections were incubated with 2% skim milk in PBS and incubated with the primary antibodies followed by incubation with fluorescence-conjugated secondary antibody. Images were captured using an Axioskop2 plus microscope (Zeiss) with an ORCA-ER digital camera (Hamamatsu Photonics, Shizuoka, Japan) and AquaCosmos software (Hamamatsu Photonics).

Cell Preparation

Single-cell suspensions were prepared from E14.5 mice embryos and from

TABLE 1. Markers and Oligonucleotides Used in This Study

Symbol	Description	GenBank		Sequence
Pan-endothelial markers				
Flk-1	fetal liver kinase 1 (VEGFR2)	—	—	—
CD34	CD34 antigen	—	—	—
CD31	platelet/endothelial cell adhesion molecule 1	NM_001032378.1	Sense	5′- GTC ATG GCC GTC GAG TA -3′
			Antisense	5′- CTC CTC GGC ATC TTG CTG AA -3′
VE-Cad	vascular endothelial cadherin	NM_009868.3	Sense	5′- CAT CCG TGT GAC AGC AGT GG -3′
			Antisense	5′- GTC TTC AGG CAC CGA AAA TGT G -3′
VWF	Von Willebrand factor homolog	NM_011708.3	Sense	5′- GTG GTG GGC ATG ATG GAG AGG TTA -3′
			Antisense	5′- GCA AGG TCA CAG AGG TAG CTG ACT -3′
Lymphatic EC markers				
Pdpn	podoplanin	NM_010329.2	Sense	5′- GTG CCA GTG TTG TTC TGG GT -3′
			Antisense	5′- TCT GTT GTC TGC GTT TCA TCC -3′
SLC	secondary lymphoid chemokine	NM_023052.1	Sense	5′- GAT GAT GAC TCT GAG CCT CC -3′
			Antisense	5′- CTC TTG AGG GCT GTG TCT GT -3′
Flt4	FMS-like tyrosine kinase 4 (VEGFR3)	NM_008029.1	Sense	5′- AGA TGC AGC CGG GCG CTG CGC T -3′
			Antisense	5′- TAG GCT GTC CCC GGT GTC AAT C-3′
Lyve-1	lymphatic vessel endothelial hyaluronan receptor-1	NM_053247.4	Sense	5′- TTC CTC GCC TCT ATT TGG AC -3′
			Antisense	5′- ACG GGG TAA AAT GTG GTA AC -3′
Hepatic sinusoidal EC markers				
Stab2	stabilin-2	NM_138673.1	Sense	5′- GCA CCA CCT CAC TAA TGT CAA -3′
			Antisense	5′- CCC AAG AGG GTC ACT GTT CT -3′
F8	coagulation factor VIII	NM_007977.1	Sense	5′- AAA GAA GGC AGT CTC TCC AAA -3′
			Antisense	5′- GGA ACT GCC CAA GAT CTA TCA -3′
FcγR2b	Fc receptor, IgG, low affinity IIb	NM_001077189.1	Sense	5′- TGT GGA CAG CCG TGC TAA AT -3′
			Antisense	5′- CAG CAG CCA GTC AGA AAT CA -3′
Hepatoblast marker				
Liv2	—	—	—	–
Pan-blood cell marker				
CD45	CD45 antigen	—	—	–
House keeping gene				
Actb	actin, beta, cytoplasmic	NM_007393.1	Sense	5′- GAT ATC GCT GCG CTG GTC GTC -3′
			Antisense	5′- ACG CAG CTC ATT GTA GAA GGT GTG G -3′

livers and lungs from 8- to 12-week-old mice as described previously (Dong et al., 1997; Kamiya et al., 1999; Nonaka et al., 2004; Morisada et al., 2005). Briefly, E14.5 livers and the upper half of the bodies were treated with enzyme-based dissociation buffer (liver digest medium, Invitrogen). Adult livers were perfused in situ by means of the portal vein with 0.05% collagenase type IV (Sigma-Aldrich, St. Louis, MO). NPCs were separated from hepatocytes by low-speed centrifugation (Seglen, 1976). Adult lungs were treated with 0.05% collagenase type IV (Sigma-Aldrich). After digestion, cells were filtered through a 70-μm cell strainer [Becton Dickinson and Company (BD), Franklin Lakes, NJ], washed, resuspended in 30% Percoll (GE Healthcare), and layered on Lympholyte-M (Cedarlane Laboratories Ltd., ON, Canada). Banded cells were harvested, washed, and counted.

Flow Cytometry

Cells were blocked with an anti-mouse CD16/32 mAb, costained with fluorescein- and biotin-conjugated antibodies, washed, and incubated with APC-conjugated streptavidin. Dead cells were stained with propidium iodide. Labeled cells were analyzed with a FACSCalibur flow cytometer (BD Biosciences) and separated using a FACSVantage (BD Biosciences).

RT-PCR Analysis

RNA was extracted from sorted HSECs, LECs, and BECs using a High Pure RNA Isolation Kit (F. Hoffmann-La Roche Ltd., Basel, Switzerland). First-strand cDNA was synthesized using SuperScript III reverse transcriptase (Invitrogen) and random hexamer primers. The thermal cycle (denaturation at 94°C for 15 sec, annealing at an appropriate temperature for each pair of primers for 15 sec and extension at 72°C for 15 sec) was repeated 35 times. The primers used are shown in Table 1.

Cell Culture

Cells were cultured at 37°C in a humidified atmosphere containing 5% CO_2. Freshly isolated ECs were suspended in EGM-2 medium (Cambrex Corporation, East Rutherford, NJ) supplemented with 2% fetal bovine serum and an endothelial growth supplement (EGM-2 SingleQuots, Cambrex) and plated onto fibronectin-coated dishes. After 1 day of incubation, cells were incubated for 3 hr with DiI-Ac-LDL (Biomedical Technologies, Inc., Stoughton, MA), at a final concentration of 5 μg/ml. Cells were washed with PBS, fixed with 4% PFA, incubated with 2% skim milk in PBS, and immunostained with anti-

mouse Stab2 mAb. Images were captured using an Ecripse TE300 microscope (Nikon) with an ORCA-ER digital camera (Hamamatsu Photonics) and an AquaCosmos software (Hamamatsu Photonics). To assess the endocytotic activity of ECs, the DiI fluorescence intensity was quantified in each image using AquaCosmos software (Hamamatsu Photonics). The number of Hoechst-stained nuclei representing the number of cells was counted and the DiI fluorescence intensity per cell was calculated.

ACKNOWLEDGMENTS

The authors thank Drs. T. Watanabe and H. Nishina for providing us with anti-Liv2 antibody, Drs. N. Fujita and T. Tsuruo for anti-Pdpn antibody, and Drs. Y. Oike and T. Suda for BaF3/Lyve-1 cells. We thank A. Hirata and S. Saito for flow cytometry. We are grateful to Drs. Y. Morikawa, T. Itoh, M. Takeuchi, and all the members of Laboratory of Cell Growth and Differentiation for technical assistance and helpful discussions. This work was supported in part by Grants-in-Aid for Scientific Research and Special Coordination Funds from the Ministry of Education, Culture, Sports, Science and Technology, the CREST program of Japan Science and Technology and Ministry of Health, Labour and Welfare, Japan.

REFERENCES

Adachi H, Tsujimoto M. 2002. FEEL-1, a Novel scavenger receptor with in vitro bacteria-binding and angiogenesis-modulating activities. J Biol Chem 277: 34264–34270.

Aird WC. 2003. Endothelial cell heterogeneity. Crit Care Med 31:S221–S230.

Banerji S, Ni J, Wang SX, Clasper S, Su J, Tammi R, Jones M, Jackson DG. 1999. LYVE-1, a new homologue of the CD44 glycoprotein, is a lymph-specific receptor for hyaluronan. J Cell Biol 144:789–801.

Bonder CS, Norman MU, Swain MG, Zbytnuik LD, Yamanouchi J, Santamaria P, Ajuebor M, Salmi M, Jalkanen S, Kubes P. 2005. Rules of recruitment for Th1 and Th2 lymphocytes in inflamed liver: a role for alpha-4 integrin and vascular adhesion protein-1. Immunity 23:153–163.

Braet F, Wisse E. 2002. Structural and functional aspects of liver sinusoidal endothelial cell fenestrae: a review. Comp Hepatol 1:1.

Buttler K, Kreysing A, von Kaisenberg CS, Schweigerer L, Gale N, Papoutsi M, Wilting J. 2006. Mesenchymal cells with leukocyte and lymphendothelial characteristics in murine embryos. Dev Dyn 235: 1554–1562.

Carmeliet P. 2003. Angiogenesis in health and disease. Nat Med 9:653–660.

Carreira CM, Nasser SM, di Tomaso E, Padera TP, Boucher Y, Tomarev SI, Jain RK. 2001. LYVE-1 is not restricted to the lymph vessels: expression in normal liver blood sinusoids and down-regulation in human liver cancer and cirrhosis. Cancer Res 61:8079–8084.

Cleaver O, Melton DA. 2003. Endothelial signaling during development. Nat Med 9:661–668.

Couvelard A, Scoazec JY, Dauge MC, Bringuier AF, Potet F, Feldmann G. 1996. Structural and functional differentiation of sinusoidal endothelial cells during liver organogenesis in humans. Blood 87: 4568–4580.

Dong QG, Bernasconi S, Lostaglio S, De Calmanovici RW, Martin-Padura I, Breviario F, Garlanda C, Ramponi S, Mantovani A, Vecchi A. 1997. A general strategy for isolation of endothelial cells from murine tissues. Characterization of two endothelial cell lines from the murine lung and subcutaneous sponge implants. Arterioscler Thromb Vasc Biol 17:1599–1604.

Enzan H, Himeno H, Hiroi M, Kiyoku H, Saibara T, Onishi S. 1997. Development of hepatic sinusoidal structure with special reference to the Ito cells. Microsc Res Tech 39:336–349.

Falkowski M, Schledzewski K, Hansen B, Goerdt S. 2003. Expression of stabilin-2, a novel fasciclin-like hyaluronan receptor protein, in murine sinusoidal endothelia, avascular tissues, and at solid/liquid interfaces. Histochem Cell Biol 120: 361–369.

Fraser JR, Alcorn D, Laurent TC, Robinson AD, Ryan GB. 1985. Uptake of circulating hyaluronic acid by the rat liver. Cellular localization in situ. Cell Tissue Res 242:505–510.

Fraser JR, Dahl LB, Kimpton WG, Cahill RN, Brown TJ, Vakakis N. 1989. Elimination and subsequent metabolism of circulating hyaluronic acid in the fetus. J Dev Physiol 11:235–242.

Gouysse G, Couvelard A, Frachon S, Bouvier R, Nejjari M, Dauge MC, Feldmann G, Henin D, Scoazec JY. 2002. Relationship between vascular development and vascular differentiation during liver organogenesis in humans. J Hepatol 37: 730–740.

Gualdi R, Bossard P, Zheng M, Hamada Y, Coleman JR, Zaret KS. 1996. Hepatic specification of the gut endoderm in vitro: cell signaling and transcriptional control. Genes Dev 10:1670–1682.

Hansen B, Longati P, Elvevold K, Nedredal GI, Schledzewski K, Olsen R, Falkowski M, Kzhyshkowska J, Carlsson F, Johansson S, Smedsrod B, Goerdt S, McCourt P. 2005. Stabilin-1 and stabilin-2 are both directed into the early endocytic pathway in hepatic sinusoidal endothelium via interactions with clathrin/AP-2, independent of ligand binding. Exp Cell Res 303:160–173.

Ikeda Y, Terashima T. 1997. Expression of reelin, the gene responsible for the reeler mutation, in embryonic development and adulthood in the mouse. Dev Dyn 210:157–172.

Irjala H, Elima K, Johansson EL, Merinen M, Kontula K, Alanen K, Grenman R, Salmi M, Jalkanen S. 2003. The same endothelial receptor controls lymphocyte traffic both in vascular and lymphatic vessels. Eur J Immunol 33:815–824.

Kamiya A, Kinoshita T, Ito Y, Matsui T, Morikawa Y, Senba E, Nakashima K, Taga T, Yoshida K, Kishimoto T, Miyajima A. 1999. Fetal liver development requires a paracrine action of oncostatin M through the gp130 signal transducer. EMBO J 18:2127–2136.

Kato Y, Sasagawa I, Kaneko M, Osawa M, Fujita N, Tsuruo T. 2004. Aggrus: a diagnostic marker that distinguishes seminoma from embryonal carcinoma in testicular germ cell tumors. Oncogene 23: 8552–8556.

Kaufman MH. 1995. The atlas of mouse development. New York: Academic Press.

Kitamura T, Onishi M, Kinoshita S, Shibuya A, Miyajima A, Nolan GP. 1995. Efficient screening of retroviral cDNA expression libraries. Proc Natl Acad Sci U S A 92:9146–9150.

Knolle PA, Limmer A. 2003. Control of immune responses by scavenger liver endothelial cells. Swiss Med Wkly 133:501–506.

Lalor PF, Lai WK, Curbishley SM, Shetty S, Adams DH. 2006. Human hepatic sinusoidal endothelial cells can be distinguished by expression of phenotypic markers related to their specialised functions in vivo. World J Gastroenterol 12:5429–5439.

Lammert E, Cleaver O, Melton D. 2003. Role of endothelial cells in early pancreas and liver development. Mech Dev 120:59–64.

LeCouter J, Moritz DR, Li B, Phillips GL, Liang XH, Gerber HP, Hillan KJ, Ferrara N. 2003. Angiogenesis-independent endothelial protection of liver: role of VEGFR-1. Science 299:890–893.

Matsumoto K, Yoshitomi H, Rossant J, Zaret KS. 2001. Liver organogenesis promoted by endothelial cells prior to vascular function. Science 294:559–563.

Morisada T, Oike Y, Yamada Y, Urano T, Akao M, Kubota Y, Maekawa H, Kimura Y, Ohmura M, Miyamoto T, Nozawa S, Koh GY, Alitalo K, Suda T. 2005. Angiopoietin-1 promotes LYVE-1-positive lymphatic vessel formation. Blood 105:4649–4656.

Morita M, Qun W, Watanabe H, Doi Y, Mori M, Enomoto K. 1998. Analysis of the sinusoidal endothelial cell organization during the developmental stage of the fetal rat liver using a sinusoidal endothelial cell specific antibody, SE-1. Cell Struct Funct 23:341–348.

Nonaka H, Sugano S, Miyajima A. 2004. Serial analysis of gene expression in si-

nusoidal endothelial cells from normal and injured mouse liver. Biochem Biophys Res Commun 324:15–24.

Oliver G. 2004. Lymphatic vasculature development. Nat Rev Immunol 4:35–45.

Orkin SH. 1996. Development of the hematopoietic system. Curr Opin Genet Dev 6:597–602.

Politz O, Gratchev A, McCourt PA, Schledzewski K, Guillot P, Johansson S, Svineng G, Franke P, Kannicht C, Kzhyshkowska J, Longati P, Velten FW, Goerdt S. 2002. Stabilin-1 and -2 constitute a novel family of fasciclin-like hyaluronan receptor homologues. Biochem J 362: 155–164.

Salmi M, Koskinen K, Henttinen T, Elima K, Jalkanen S. 2004. CLEVER-1 mediates lymphocyte transmigration through vascular and lymphatic endothelium. Blood 104:3849–3857.

Samama B, Boehm N. 2005. Reelin immunoreactivity in lymphatics and liver during development and adult life. Anat Rec A Discov Mol Cell Evol Biol 285:595–599.

Sasaki K, Sonoda Y. 2000. Histometrical and three-dimensional analyses of liver hematopoiesis in the mouse embryo. Arch Histol Cytol 63:137–146.

Scoazec JY, Feldmann G. 1991. In situ immunophenotyping study of endothelial cells of the human hepatic sinusoid: results and functional implications. Hepatology 14:789–797.

Seglen PO. 1976. Preparation of isolated rat liver cells. Methods Cell Biol 13:29–83.

Smedsrod B, Pertoft H, Gustafson S, Laurent TC. 1990. Scavenger functions of the liver endothelial cell. Biochem J 266: 313–327.

Takebe Y, Seiki M, Fujisawa J, Hoy P, Yokota K, Arai K, Yoshida M, Arai N. 1988. SR alpha promoter: an efficient and versatile mammalian cDNA expression system composed of the simian virus 40 early promoter and the R-U5 segment of human T-cell leukemia virus type 1 long terminal repeat. Mol Cell Biol 8:466–472.

Tanimizu N, Nishikawa M, Saito H, Tsujimura T, Miyajima A. 2003. Isolation of hepatoblasts based on the expression of Dlk/Pref-1. J Cell Sci 116:1775–1786.

Wang HU, Chen Z-F, Anderson DJ. 1998. Molecular Distinction and Angiogenic Interaction between Embryonic Arteries and Veins Revealed by ephrin-B2 and Its Receptor Eph-B4. Cell 93:741–753.

Watanabe M, Okochi E, Sugimoto Y, Tsuruo T. 1988. Identification of a platelet-aggregating factor of murine colon adenocarcinoma 26: Mr 44,000 membrane protein as determined by monoclonal antibodies. Cancer Res 48:6411–6416.

Watanabe T, Nakagawa K, Ohata S, Kitagawa D, Nishitai G, Seo J, Tanemura S, Shimizu N, Kishimoto H, Wada T, Aoki J, Arai H, Iwatsubo T, Mochita M, Satake M, Ito Y, Matsuyama T, Mak TW, Penninger JM, Nishina H, Katada T. 2002. SEK1/MKK4-mediated SAPK/JNK signaling participates in embryonic hepatoblast proliferation via a pathway different from NF-kappaB-induced anti-apoptosis. Dev Biol 250:332–347.

Wigle JT, Harvey N, Detmar M, Lagutina I, Grosveld G, Gunn MD, Jackson DG, Oliver G. 2002. An essential role for Prox1 in the induction of the lymphatic endothelial cell phenotype. EMBO J 21: 1505–1513.

Zhou B, Weigel JA, Fauss L, Weigel PH. 2000. Identification of the Hyaluronan Receptor for Endocytosis (HARE). J Biol Chem 275:37733–37741.

p75 neurotrophin receptor is a marker for precursors of stellate cells and portal fibroblasts in mouse fetal liver

Kaori Suzuki[1,2*], Minoru Tanaka[1,2*], Natsumi Watanabe[1], Shigeru Saito[1,2], Hidenori Nonaka[1] and Atsushi Miyajima[1,2]

* These authors equally contributed to this study.
[1]Institute of Molecular and Cellular Biosciences, University of Tokyo, Tokyo, Japan; [2]Core Research for Evolutionary Science and Technology of Japan Science and Technology Agency (JST), Japan

This work was supported in part by a grant for Core Research for Evolutionary Science and Technology of Japan Science and Technology Agency (JST), a research grant from the Ministry of Education, Sports, Science and Technology, and a research grant of Ministry of Health, Labour and Welfare.

Abbreviations used in this paper: HSC, hepatic stellate cell; PF, portal fibroblast; NPC, non-parenchymal cell; IHC, imunohistochemistry; FCM, flow cytometry; RT-PCR, reverse-transcription polymerase chain reaction; TUNEL, terminal deoxynucleotidyl transferase-mediated deoxy uridine 5'-triphosphate-biotin nick-end labeling; p75NTR, p75 neurotrophin receptor; α–SMA, α-smooth muscle actin; GFAP, glial fibrillary acidic protein; NGF, nerve growth factor; Dlk, Delta-like protein; Lyve1, lymphatic vessel endothelial hyaluronan receptor 1; Flk-1, fetal liver kinase-1; CK, cytokeratin; HPRT, hypoxanthine-guanine phosphoribosyltransferase; PECAM1, platelet/endothelial cell adhesion molecule 1; ECM, extracellular matrix; STM, septum transversum mesenchyme; cDNA, complementary DNA; EGFP, enhanced green fluorescence protein; E, embryonic day; P, postnatal day; mAb, monoclonal antibody

Conflicts of interest: There are no conflicts of interest to disclose.

Corresponding author:
Minoru Tanaka
Laboratory of Cell Growth and Differentiation, Institute of Molecular and Cellular Biosciences, University of Tokyo, 1-1-1 Yayoi, Bunkyo-ku, Tokyo 113-0032, Japan.
Phone: 81-3-5841-7889.
Fax: 81-3-5841-8475.
E-mail: **tanaka@iam.u-tokyo.ac.jp**

Background & Aims: Hepatic stellate cells (HSCs) and portal fibroblasts (PFs) are two distinct mesenchymal cells in adult liver. HSCs in sinusoids accumulate lipids and express p75 neurotrophin receptor (p75NTR). HSCs and PFs play pivotal roles in liver regeneration and fibrosis. However, the roles of mesenchymal cells in fetal liver remain poorly understood. In this study, we aimed to characterize mesenchymal cells in mouse fetal liver. **Methods:** We prepared an anti-p75NTR monoclonal antibody applicable for flow cytometry and immunohistochemistry. $p75NTR^+$ cells isolated from fetal liver by flow cytometry were characterized by reverse transcription polymerase chain reaction, immunohistochemistry and cell cultivation. Lipid-containing cells were visualized by Oil-red O staining. **Results:** $p75NTR^+$ cells in fetal liver were clearly distinct from endothelial cells and showed characteristics of mesenchymal cells. At embryonic day (E) 10.5, $p75NTR^+$ cells were present at the periphery of the liver bud in close contact with endothelial cells, and spread over the liver at E11.5. With the formation of the liver architecture, they began to localize to two distinct areas, parenchymal and portal areas, and lipid-containing $p75NTR^+$ cells increased accordingly. $p75NTR^+$ cells around portal veins were adjacent to cholangiocytes and expressed Jagged1, a crucial factor for the commitment of hepatoblasts to cholangiocytes. By cultivation, $p75NTR^+$ cells exhibited features of adult HSCs with markedly increased expression of glial fibrillary acidic protein and α-smooth muscle actin. **Conclusions:** $p75NTR^+$ mesenchymal cells in fetal liver include progenitors for HSCs and PFs, and the anti-p75NTR monoclonal antibody is useful for their isolation.

Introduction

The liver consists of two types of epithelial cells, hepatocytes and cholangiocytes (biliary epithelial cells), and various non-parenchymal cells (NPCs) that include hematopoietic, endothelial, and mesenchymal cells. There are three major mesenchymal cells in the liver, i.e. hepatic stellate cells (HSCs), portal fibroblasts (PFs) and vascular smooth muscle cells residing in the walls of portal veins, arteries and central veins. HSCs, also known as Ito cells, fat-storing cells, or lipocytes, are pericytes found in the perisinusoidal space between sinusoids and hepatocytes in adult liver. Protrusions extending from HSCs wrap sinusoidal endothelial cells that constitute the sinusoidal capillary network in the liver. By contrast, PFs are present in the connective tissue around portal vessels and bile ducts. In normal liver, HSCs are in a quiescent state and contain vitamin A-rich lipid droplets, constituting the largest reservoir of vitamin A in the body,[1] whereas PFs do not store lipid droplets. While HSCs express desmin but not elastin, PFs exhibit inverse expression pattern.[2] In injured liver, HSCs become the activated and transform into myofibroblast-like cells that secrete various cytokines to contribute to liver regeneration.[3, 4] Those activated HSCs are enlarged, lack lipid droplets,[5, 6] and express α-smooth muscle actin (α-SMA).[7, 8] Upon prolonged liver injury, the transformed myofibroblast-like cells produce a large amount of extracellular matrix (ECM), leading to fibrosis.[1, 9] Similarly, the activated PFs express α-SMA and differentiate into mybofibroblasts, which are involved in the early stages of biliary fibrosis.[10, 11] Because HSCs and PFs play pivotal roles in liver repair and diseases, the nature of these intriguing cell types has been a subject of intense research. HSCs exhibit features of both mesenchymal cells and neural/neuroendocrine cells by expressing vimentin, desmin[12] and α-SMA, as well as glial fibrillary acidic protein (GFAP),[13] nestin,[14] neural cell adhesion molecule[15] and synaptophysin,[16] respectively. As HSCs exhibit mesenchymal and neuronal features, it has been postulated that their origin is related to the neuronal lineage, i.e. neural crest cells. However, Cassiman et al. reported that HSCs are not derived from the neural crest.[17] Moreover, it was recently reported that bone marrow cells become HSCs in adult liver.[18] Although the distinction between adult HSCs and PFs has now been demonstrated,[2] the nature and origin of these mesenchymal precursors remain unclear.[19]

Hepatocytes and cholangiocytes derive from hepatoblasts, which emerge from the foregut endoderm and invade into the septum transversum mesenchyme (STM) to form the liver bud.[20] It was shown that the proliferation of hepatoblasts requires endothelial cells using explant cultures from mutant mouse embryos defective in the development of endothelial cells.[21] As hepatocytes and HSCs interact intimately in adult liver and bile ducts are formed along with the portal veins consisting of endothelial cells and mesenchymal cells, they are speculated to interact at a certain stage of development. However, it still remains unknown when mesenchymal cells develop and whether they affect the proliferation and/or differentiation of hepatoblasts. As adult HSCs contain numerous vitamin A-rich lipid droplets, low density cells separated from the NPCs in normal liver by centrifugation through various density media have been used to study HSCs.[22-26] However, this method is not applicable to the preparation of fetal HSC precursors because they do not store enough lipid droplets for separation. In addition, a lack of HSC markers for cell sorting has prevented the investigation of HSCs in liver development. Therefore, little information is available on fetal HSCs and/or their precursors and their characterization requires the prospective isolation of the fetal liver cell populations. To this end, we generated many monoclonal antibodies (mAbs) against fetal liver cells and selected those that recognize cell surface proteins. One of those mAbs recognized p75 neurotrophin receptor (p75NTR), a receptor for neurotrophic factors such as nerve growth factor (NGF), brain-derived neurotrophic factor, neurotrophin 3 and neurotrophin 4/5. While p75NTR is mainly expressed in the nervous system,[27] it is also expressed in non-neural tissues, some tumor cells and normal mesenchymal precursor cells of myoid cells in testis.[28] In addition, it was previously shown that human and rat HSCs expressed p75NTR[29] and that activated HSCs expressing p75NTR undergo apoptosis in response to NGF *in vitro*.[30-32] Recently, Passino et al. reported that depletion of p75NTR in mice exacerbated liver pathology and inhibited hepatocyte proliferation *in vivo*.[33, 34] Furthermore, they showed that ligand-independent p75NTR signaling to Rho enhanced the differentiation of HSCs into regeneration-promoting cells that support hepatocyte proliferation in diseased liver. However, the expression of p75NTR in fetal liver and the nature of $p75NTR^{+}$ cells remained unknown. Here, we show

p75NTR expression in fetal liver at an early stage of development, and characterize the p75NTR$^+$ cells isolated from mouse fetal liver. Our data suggest that the p75NTR$^+$ cell population contains mesenchymal cell precursors for HSCs and PFs. Furthermore, we show that the p75NTR$^+$ cells in the periportal area could contribute to the formation of intrahepatic bile ducts in the late gestational stage.

Results

Monoclonal antibodies against mouse fetal liver cells

To characterize various cell compartments in mouse fetal liver, we immunized a rat with embryonic day (E) 14.5 liver cells and established a total of 627 hybridomas (Supplementary Figure 2). By flow cytometric analysis (FCM) and immunohistochemical analysis (IHC) of fetal liver cells using each antibody, we found that the 25-8 antibody showed a staining pattern apparently distinct from that of hepatoblasts, which were stained with anti-Delta-like protein (Dlk) antibody[35] (Figure 1A, C and D). The pattern of staining by the 25-8 antibody was similar to that of sinusoidal endothelial cells, which were stained with the anti-lymphatic vessel endothelial hyaluronan receptor 1 (Lyve1)[36] antibody (Figure 1B). However, the 25-8 antibody also stained several cells around large blood vessels (Figure 1D), suggesting that it recognized a cell type distinct from hepatoblasts and sinusoidal endothelial cells. By expression cloning of cDNA, we successfully identified p75NTR as the 25-8 antigen. To confirm the specificity of the 25-8 antibody, we expressed p75NTR cDNA or Lyve1 cDNA in Ba/F3 cells and performed FCM using the 25-8 antibody (Figure 1E). The 25-8 antibody bound Ba/F3 cells expressing p75NTR but not parental Ba/F3 cells and Ba/F3 cells expressing Lyve1, indicating that it recognized p75NTR specifically. To confirm the expression of p75NTR in adult mouse HSCs, we isolated HSCs by centrifugation through 11% Nycodenz and examined the expression of p75NTR by FCM using the 25-8 antibody (Figure 1F). Almost all the lipid-storing cells in mouse liver expressed p75NTR. Reverse transcription polymerase chain reaction (RT-PCR) analysis also showed that HSCs isolated by density centrifugation expressed p75NTR as well as GFAP, a well-known marker for HSCs (Figure 1G).

Localization of p75NTR$^+$ cells in the liver

In contrast to the expression of p75NTR in adult liver cells, that in fetal liver cells had not been studied. In the early stage around E9, the pre-hepatic cells delaminate from the foregut and migrate as cords into the surrounding STM. However, it remained unknown whether p75NTR$^+$ cells are present at the early stage of mouse liver development. To address this issue, we performed IHC of mouse liver at E10.5, E11.5 and E12.5. Hepatoblasts were clearly detected by anti-Dlk antibody at these stages (Figure 2A-F). Consistent with a previous study,[21] fetal liver kinase-1 (Flk-1)$^+$ endothelial cells were present in E10.5 liver and formed primitive sinusoids (Figure 2A and J). Interestingly, p75NTR$^+$ cells were found at the periphery of liver the primordium adjacent to the STM and the part of the primitive sinusoids (Figure 2J). Then, p75NTR$^+$ cells were observed uniformly throughout the liver at E11.5 and E12.5 (Figure 2E and F). In addition, IHC showed that a majority of the p75NTR$^+$ cells were in contact with Flk-1$^+$ endothelial cells as well as Dlk$^+$ hepatoblasts (Figure 2D-K). Although IHC with 25-8 antibody showed a pattern similar to that of sinusoidal endothelial cells (Figure 1), these results strongly suggest that p75NTR$^+$ cells and endothelial cells are distinct populations and interact with each other at an early stage in the development of liver prior to vascular function.

Characterization of p75NTR$^+$ cells in fetal liver

To characterize the p75NTR$^+$ cells in E11.5 mouse liver, we performed FCM using the 25-8 antibody and revealed that approximately 1.5% of all fetal liver cells expressed p75NTR (Figure 3B). Neither CD45 nor TER119 was expressed in p75NTR$^+$ cells, indicating that they were a non-hematopoietic lineage (Figure 3C and D). Consistent with the result of IHC in Figure 2, p75NTR$^+$ cells were negative for Lyve1, PECAM1 and Flk-1 by FCM, confirming that p75NTR$^+$ cells were not endothelial cells (Figure 3E and Supplementary Figure 3). This result is in accordance with numerous studies that have characterized the expression of p75NTR in the mouse, rat and human liver and have shown that HSCs are major source of p75NTR in the adult liver.[29, 30, 33] Considering the localization of mesenchymal cells in adult liver, two distinct populations of p75NTR$^+$ cells in

E14.5 liver might correspond to HSCs and PFs in developing liver. To address this possibility, we sorted p75NTR$^+$ cells from fetal livers at E11.5 and E14.5, and analyzed the expression of known mesenchymal markers by RT-PCR (Figure 3F). Vimentin, desmin and α-SMA were expressed in p75NTR$^+$ cells at E11.5. These markers were expressed abundantly in p75NTR$^+$ cells and poorly in p75NTR$^-$ cells at E14.5. These results clearly indicated that p75NTR$^+$ cells in fetal liver were mesenchymal cells. While GFAP was detected in adult HSCs and E14.5 p75NTR$^+$ cells by RT-PCR, it was not expressed in E11.5 p75NTR$^+$ cells (Figure 1G and 3F), suggesting that GFAP is not expressed in HSC progenitors and hence it may be a good marker for the differentiation of liver mesenchymal cell populations.

p75NTR is a marker for HSC progenitors

To reveal the expression patterns of p75NTR and GFAP in liver development, we performed IHC of the liver at various developmental stages. GFAP was detected in the p75NTR$^+$ cells at E14.5 and the signal was intensified towards adulthood, whereas it was rarely observed in p75NTR$^+$ cells at E11.5 (Figure 4A). Therefore, p75NTR expression precedes GFAP expression in HSCs and marks their progenitors at the early stage of liver development. Although α-SMA has been considered as a marker for activated HSCs and PFs, it was detected in hepatic p75NTR$^+$ cells at E11.5 and E14.5 by RT-PCR (Figure 3F). IHC showed that α-SMA was not expressed in p75NTR$^+$ cells in the parenchymal area at E11.5, whereas it was expressed in p75NTR$^+$ cells around large blood vessels (Figure 4B). These results suggest that HSC precursors and perivascular mesenchymal cells in fetal liver are distinguishable by the expression of α-SMA.

To further investigate p75NTR$^+$ cells, we isolated and cultured p75NTR$^+$ cells from E11.5 liver. IHC showed that GFAP was not detected in p75NTR$^+$ cells at day 1 of cultivation in gelatin-coated dishes, but it was detected in approximately 20% of cultured cells at day 5 (Figure 4C). While p75NTR$^+$ cells expressed a very low level of α-SMA at day 1 on non-coated dishes, all p75NTR$^+$ cells showed a flattened, myofibroblast-like shape with strong expression of α-SMA, characteristic of activated HSCs after longer cultivation (Figure 4D). Thus, p75NTR$^+$ cells in E11.5 liver acquired characteristics of adult HSCs, PFs and potentially other mesenchymal cells *in vitro*.

As the accumulation of lipid droplets is a characteristic feature of adult HSCs, we investigated lipid accumulation in p75NTR$^+$ cells by Oil-red O staining at various developmental stages. While lipid-containing p75NTR$^+$ cells were rarely observed in E11.5 liver, approximately 12% of p75NTR$^+$ cells contained lipid droplets at E14.5 and one third at E18.5 (Figure 4E). These results indicated that immature HSC precursors are in the p75NTR$^+$ cell population in fetal liver. Based on these results, we concluded that p75NTR is the earliest marker for HSC progenitors and that p75NTR$^+$ cells acquire the characteristics of mature HSCs.

Since it has been reported that activated HSCs expressing p75NTR undergo apoptosis in response to NGF *in vitro*, we examined apoptosis in p75NTR$^+$ mesenchymal cells in the fetal liver. Double immunofluorescence of *in situ* TUNEL and anti-p75NTR antibody at various developmental stages revealed that apoptotic cells were rarely detected in E12.5 and E14.5 liver. Although there were some apoptotic cells in E16.5 liver, they were negative for p75NTR, suggesting p75NTR not to be involved in apoptosis at the fetal stage of liver development (Supplementary Figure 4).

Heterogeneity of p75NTR$^+$ cells and a possible role of periportal p75NTR$^+$ cells in bile duct formation

While p75NTR$^+$ cells were present uniformly throughout the liver in the early stages, E11.5 and E12.5, they were found in both parenchymal and perivascular areas at E14.5 (Figure 1C and D). In the mid-to-late stages of liver development, the intrahepatic bile ducts are formed from hepatoblasts around the portal veins.[37] Although the cells responsible for the commitment of hepatoblasts to cholangiocytes were expected to be present in the periportal region, the exact cell type remained unknown. Because p75NTR was strongly expressed in the periphery of portal veins, we hypothesized that p75NTR$^+$ cells contributed to the differentiation of hepatoblasts into cholangiocytes. To test this possibility, we performed IHC of liver with anti-p75NTR and anti-cytokeratin (CK)19 antibodies at different stages. At E14.5, intense label of p75NTR was detected around large blood vessels and some CK19-expressing cells, which are committed to the

cholangiocytic lineage, were in contact with p75NTR$^+$ cells (Figure 5A). Interestingly, ductal plates and bile ducts around the portal vein were located on the outside of p75NTR$^+$ cells at E16.5 and postnatal stages, respectively (Figure 5B, C and D). This result strongly suggested that p75NTR$^+$ cells play a role in the differentiation of hepatoblasts into cholangiocytes. In fact, the cells with an intense p75NTR signal were in contact with CK19$^+$ cells, whereas no CK19$^+$ cells were found in the region with a faint p75NTR signal (Figure 5B; arrow and arrowhead). Impairment of Jagged1, a ligand for the Notch receptor, is responsible for Alagille syndrome, patients with which show a paucity in the development of intrahepatic bile ducts.[38-40] We previously showed that Notch2 and Jagged 1 were expressed in hepatoblasts and the periportal area, respectively. Activation of Notch signaling in hepatoblasts enhanced cholangioctic differentiation. These results suggested that the activation of Notch2 by Jagged1 induces the differentiation of hepatoblasts into cholangiocytes [40, 41]. As it remained unknown which cells in the periportal area express Jagged1, we performed FCM of E14.5 liver cells with anti-p75NTR and anti-Jagged1 antibodies and found that some p75NTR$^+$ cells expressed Jagged1 (Fig. 5E). Furthermore, the p75NTR$^+$ cells but not p75NTR$^-$ cells sorted from E14.5 liver expressed Jagged1 as determined by immunostaining and RT-PCR (Fig. 5F, G). The presence of p75NTR$^+$Jagged1$^+$ cells in E14.5 liver suggested that the differentiation of periportal p75NTR$^+$ cells precedes the formation of ductal plates. Actually, anti-Jagged1 antibody stained p75NTR$^+$ cells in the periportal region, but not the other region at E14.5 (Figure 5H). These findings strongly suggested that portal p75NTR$^+$ cells contribute to the biliary differentiation of adjacent hepatoblasts and bile duct formation.

Discussion

Since hepatic mesenchymal cells including HSCs change their characteristics depending on their location and activation, they are considered a heterogeneous cell population. Mesenchymal cells near the portal vein are fibroblastic and produce more ECM than those in sinusoids away from the portal area. Additionally, the expression levels of HSC markers such as desmin, vimentin, and α-SMA vary dependent on the activation state. As HSCs accumulate lipid droplets, they can be isolated by density. However, it is not possible to isolate the HSC precursors and transformed myofibroblasts, which lack lipid droplets, and hence studies of HSC development in fetal liver had been restricted to mostly histological and microscopic observations.[42, 43] In this paper, we demonstrated that p75NTR can be used for the identification and isolation of at least two types of mesenchymal cells from fetal liver, i.e. HSC precursors and portal fibroblastic cells. Interestingly, the p75NTR$^+$ cells isolated from E11.5 liver did not express GFAP but did express it in culture, indicating that GFAP is a good marker with which to evaluate the differentiation of HSCs. Furthermore, p75NTR$^+$ cells rarely contained lipid droplets at E11.5 but they accumulated lipids at a later stage. These results indicate that p75NTR marks HSC progenitors at an early stage of liver development.

Previous studies suggested that cells or factors in the portal area contributed to the differentiation of hepatoblasts into cholangiocyes and formation of bile ducts.[44] We found that a subpopulation of p75NTR$^+$ cells in E14.5 liver expressed Jagged1 and that these cells were mostly located in the periportal area where bile ducts are formed. We previously showed that Notch2 was expressed in hepatoblasts and Jagged1 was expressed in the periportal region.[41] Furthermore, activation of the Notch pathway by forced expression of the Notch intracellular domain in Dlk$^+$ hepatoblasts enhanced cholangiocyte differentiation but suppressed hepatocyte differentiation. While these results indicated that Jagged1+ cells in the periportal area instruct hepatoblasts to become cholangiocytes, it remained unknown which cells in the periportal area expressed Jagged1. The results in this paper clearly show that p75NTR+ mesenchymal cells express Jagged1 and hence induce the differentiation of hepatoblasts into cholangiocytes.

While p75NTR$^+$ cells may be heterogeneous at the onset of liver development, it is also possible that p75NTR$^+$ cells are common precursors for both Jagged1$^+$ periportal cells and Jagged1$^-$ perisinusoidal HSCs at an earlier stage. In this case, instructive signals to express Jagged1 may be provided by the cells around the portal vein. As it was shown that a gradient of Transforming growth factor β in the periportal region might be a cue for the development of bile ducts,[45] it is tempting to speculate that such factors are involved in the expression of Jagged1 in the periportal region. Recently, Passino et al. reported that the total numbers of

desmin$^+$ HSCs in wild-type and p75NTR-deficient adult mice were similar, suggesting that p75NTR does not affect HSC development.[33] However, they also reported that the intracellular domain of p75NTR was involved in the activation of adult HSCs, i.e. induction of α-SMA expression. Likewise, p75NTR may be involved in the strong expression of α-SMA in the p75NTR+ cells around large blood vessels during liver development. Further studies on sorted cells using anti-p75NTR antibody should help us to better understand the mechanism regulating the differentiation of hepatic mesenchymal cells as well as intrahepatic bile duct specification. In conclusion, p75NTR is an excellent marker for the identification and purification of mesenchymal cell precursors including HSCs and PFs.

Materials and Methods

Mice

C57BL/6 mice (Nihon SLC, Japan) were used for all the experiments. All experiments with animals were approved by the institutional animal care and use committee of the University of Tokyo.

Generation of mAbs and identification of their antigens

Anti-p75NTR (clone 25-8), anti-Dlk and anti-Lyve1 mAbs were generated by immunization of a rat with mouse fetal hepatic cells. Hepatic cells were dissociated by collagenese from E14.5 mouse liver,[46] and used for the immunization after the depletion of CD45$^+$/TER119$^+$ hematopoietic cells by magnetic beads (Dynabeads; Invitrogen Corp., CA). Hybridomas were established by the fusion of lymphocytes and P3X myeloma cells with polyethyleneglycol as described previously.[47] To identify antigens, retrovirus-mediated expression cloning was performed as described previously.[48] To confirm the specific reactivity, mouse p75NTR, Dlk or Lyve1 cDNA were expressed in Ba/F3 cells by a retroviral vector, pMX/IRES-GFP vector (pMIG)[49] and the transfectants were stained with each purified antibody, and analyzed with FCM.

Antibodies

In addition to the mAbs we prepared, we used two kinds of polyclonal antibodies against p75NTR; rabbit anti-mouse p75NTR polyclonal antibody (AB1554) (CHEMICON International inc., Temecula, CA) (used in Figures 2, 5F and H) and goat anti-mouse NGFR/TNFRSF16 polyclonal antibody (AF1557) (R&D Systems, Minneapolis, MN) (used in Figures 4, 5A-D and 6) for immunocytochemistry and IHC. The characteristics of each anti-p75NTR antibody and information of the other antibodies used are described in Supplementary Figure 1 and Supplementary Materials and Methods.

Preparation of liver cells and flow cytometry

Single-cell suspensions were prepared from mouse E11.5 and E14.5 liver according to the method of Kamiya et al.[46] Aliquots of cells were blocked with anti-FcR antibody, co-stained with fluorescein- and biotin-conjugated antibodies, washed, incubated with allophycocyamin-conjugated streptavidin, and analyzed by FACSCalibur (BD). Dead cells were excluded by propidium iodide staining. Cell sorting was performed by FACSVantage (BD), or by autoMACS (Miltenyi Biotec GmbH, Germany) after incubation with biotinylated anti-p75NTR antibody (25-8) and streptavidin-microbeads. A single cell suspension and stellate cells from adult liver were prepared as described previously.[50] In short, liver cells were isolated by the two-step collagenase perfusion method. The cell suspension was centrifuged at 500 rpm for 1 minute twice. NPCs were prepared from the supernatant and subjected to 11% Nycodenz gradient centrifugation to collect stellate cells.[18]

Immunohistochemistry and immunocytochemistry

Frozen sections (5μm) were prepared with a Microm HM505E cryostat (MICROM International GmbH, Germany) and mounted on glass slides coated with aminopropylsilane (Matsunami glass Ind. Ltd., Japan) They were fixed with 4% paraformaldehyde in phosphate-buffered saline (PBS) or in cold acetone. Cells were permeabilized with a 0.2% Triton-X solution if required. After a blocking procedure with 5% skim milk in PBS,

sections were incubated with primary antibodies, followed by biotin- or fluorescent- conjugated secondary antibody. To visualize signals, sections were treated with 0.3% H_2O_2 in PBS after fixation, and a Vectastain ABC kit (Vector Laboratories, CA) and 3,3-diaminobenzidine tetrahydrochloreide were used. Counter staining was performed with Hematoxylin or Hoechst. For immunocytochemistry, cells were mounted on glass slides with Shandon Cytospin (Thermo Fisher Scientific Inc., MA).

RNA Extraction and RT-PCR

Total RNA was extracted with TRIZOL (Invitrogen). Total RNA and random hexamer primers were used to synthesize cDNA using SuperScript III reverse transcriptase (Invitrogen). The PCR primers used are described in Supplementary Materials and Methods.

Cell culture

Cells were cultured at 37°C in a humidified atmosphere containing 5% CO_2. p75NTR$^+$ cells isolated from E11.5 liver by auto MACS were suspended in Dulbecco's modified eagle's medium (Invitrogen) supplemented with 10% fetal bovine serum and antibiotics. For the induction of GFAP expression, cells were cultured on gelatin-coated plastic dishes in the presence of oncostatin M (10μg/ml). For activation, cells were cultured on non-coated plastic dishes.

Oil-red O staining

p75NTR$^+$ cells were collected from E11.5, E14.5, E18.5 and neonatal liver with autoMACS. The cells were mounted on glass slides and stained with Oil-red O staining solution.[51]

Figure legends

Figure 1. Expression of p75NTR in fetal mesenchymal cells and adult HSCs. Frozen sections of E14.5 liver, stained with anti-Dlk antibody (A), anti-Lyve1 antibody (B), and anti-p75NTR (25-8) antibody (C, D) (Original magnification; 200X). (E) FCM of Ba/F3 cells (left panel), Ba/F3 cells expressing p75NTR and EGFP (middle panel), and Ba/F3 cells expressing Lyve1 and EGFP (right panel) with the 25-8 antibody. (F) FCM of adult HSCs with the 25-8 antibody. (G) Expression of p75NTR and GFAP in HSCs and the other cells prepared from adult mouse NPCs by centrifugation through 11% Nycodenz.

Figure 2. IHC of liver sections at the early stage of liver development.
Liver sections were prepared from E10.5 (A, D, G, J), E11.5 (B, E, H, K), and E12.5 (C, F, I) embryos. Hepatoblasts were detected as a green color with anti-Dlk antibody (A-F). Endothelial cells were stained red with anti-Flk-1 antibody (A-C, G-K). p75NTR$^+$ cells were stained red (D-F) or green (G-K) with anti-p75NTR antibody (D-F). Image with confocal microscopy (K). (Original magnification; 200X:A-I, 100X:J, 400X:K)

Figure 3. Characterization of p75NTR$^+$ cells in fetal liver. (A) FCM of E11.5 liver cells with anti-p75NTR (25-8) antibody and lineage markers. TER119 and CD45 for hematopoietic cells and Lyve1 for sinusoidal endothelial cells. (B) Expression profiles of mesenchymal cell marker genes in p75NTR$^+$ cells sorted from E11.5 and E14.5 livers.

Figure 4. Differentiation of p75NTR$^+$ cells to HSCs in vivo and in vitro
(A) IHC of frozen sections of E11.5, E14.5, neonate and adult livers with anti-GFAP antibody (green) and anti-p75NTR antibody (red). (B) IHC of frozen sections of E11.5 livers with anti-p75NTR antibody (red) and anti-αSMA antibody (green). (C, D) *In vitro* culture and immunostaining of p75NTR$^+$ cells sorted from E11.5 fetal liver. p75NTR$^+$ cells were seeded on a gelatin-coated dish (C) or non-coated dish (D). (C) Immunostaining of attached cells with anti-GFAP antibody 1 day and 5 days after culture. Approximately 20% of the cells were positive for GFAP. (D) Immunostaining of cultured cells with anti-α-SMA antibody 1 day and 7 days after culture. (E) Ratio of lipid-containing cells in p75NTR$^+$ cells. (Original magnification; X200)

Figure 5. Characterization of p75NTR$^+$ cells around portal veins. (A-D) frozen sections of E14.5 (A), E16.5 (B) and postnatal day 1 (P1) (C, D) livers were stained with anti-p75NTR antibody (red) and anti-CK19 antibody (green). Cholangiocytic CK19$^+$ cells are located on the outside of portal p75NTR$^+$ cells with intense labeling (arrowhead), whereas no CK19$^+$ cells are located on the outside of a faint signal (arrow) (Original magnification; 200X: A-C, X400: D). (E) FCM of E14.5 liver cells with anti-p75NTR antibody and anti-Jagged1 antibody. (F) IHC of dispersed fetal liver cells with anti-p75NTR antibody (green) and anti-Jagged1 antibody (red). (G) Expression of Jagged1 in p75NTR$^+$ and p75NTR$^-$ cells of E14.5 liver by RT-PCR. (H) IHC of E14.5 liver with anti-p75NTR antibody (green) and anti-Jagged1 antibody (red). (Original magnification; X400)

Supplementary materials and methods

Antibodies

The primary antibodies used were rat anti-mouse Dlk, rat anti-mouse Lyve1 mAbs (generated in our laboratory as mentioned in the text); rat anti-mouse CD16/32 (Fc gamma receptor III, FcR) mAb, fluorescein isothiocyanate (FITC)-conjugated rat anti-mouse CD45 mAb and FITC–conjugated anti-mouse TER119 mAb (BD Biosceiences Pharmingen, San Diego, CA); goat anti-mouse vascular endothelial growth factor receptor-2 (Flk-1) polyclonal antibody (R&D); rabbit anti-human α-SMA polyclonal antibody (ab5694) (Abcam plc, Cambridge, UK); rabbit anti-cow GFAP polyclonal antibody (Z0334) (DakoCytomation, Denmark); rabbit anti-mouse CK19 polyclonal antibody{Tanimizu, 2003 #162}; and goat anti-rat Jagged1 polyclonal antibody (sc-6011) (Santa Cruz Biotechnology Inc., Santa Cruz, CA). Antibodies against p75NTR (25-8), Dlk and Lyve1 were biotinylated using Amersham ECL Protein Biotinylation Module (GE Healthcare UK Ltd.,Buckinghamshire, UK). The secondary antibodies and reagents used were FITC-conjugated rabbit anti-goat IgG (Pierce Biotechnology, Rockfold, IL); Alexa Fluor 488-conjugated donkey anti-rabbit IgG, Alexa Fluor 488-conjugated donkey anti-rat IgG, and Alexa Fluor 594-conjugated chick anti-goat IgG (Invitrogen); biotinylated rabbit anti-rat IgG (Vector Laboratories, Burlingame, CA); and allophycocyamin-conjugated streptavidin (Invitrogen).

PCR primers

α-SMA (5'-gtatgtggctattcaggctg-3' and 5'-cttctgcatcctgtcagcaa-3'), desmin (5'-tcgacgtggagcgtgacaacc-3' and 5'-cgcaatgttgtcctgatagcc-3'), GFAP (5'-agtccctagagcggcaaatgc-3' and 5'- ccttctgacacggatttggt-3'), Jagged1 (5'-cagtggactggcaagacttg-3' and 5'-tgcagctgtcaatcacttcg-3'), p75NTR (5'-gcagcgcagcgcagctcagc-3' and 5'-ctctgggcactcttcacaca-3'), vimentin (5'-cgcagcctctattcctcatc-3' and 5'-agccacgctttcatactgct-3'), HPRT (5'-ccagcaagcttgcaaccttaacca-3' and 5'-gactgaaagacttgctcgag-3').

Double immunofluorescence of *in situ* TUNEL and anti-p75NTR antibody

Immunostaining and TUNEL staining were simultaneously performed as follows. After a blocking procedure with 5% skim milk in PBS, tissue sections were incubated with anti-p75NTR antibody, washed with PBS, and incubated with TdT enzyme solution (in situ apoptosis detection kit; TaKaRa Bio Inc., Japan) and secondary antibody.

Supplementary figure legends

Supplementary Figure 1

Comparison of rat anti-p75NTR (25-8) mAb, rabbit anti-p75 NGFR polyclonal antibody and goat anti-NGFR/TNFRSF16 polyclonal antibody by immunocytochemistry and FCM. While all antibodies were useful for immunocytechemistry, the 25-8 antibody, but not the other polyclonal antibodies were useful for FCM.

Supplementary Figure 2

Among 627 antibodies generated, 262 recognized cell surface molecules on FCM using fetal liver cells. Among them, 36 antibodies recognized Dlk. We then performed IHC of E14.5 liver sections and found that 72

antibodies were applicable for immunostaining. Among them, 6 antibodies including the 25-8 antibody showed staining patterns apparently distinct from that of hepatoblasts, which were stained with anti-Dlk antibody (Figure 1A, C and D).

Supplementary Figure 3

FCM of E11.5 liver cells with anti-p75NTR (25-8) antibody and an endothelial lineage marker, anti-PECAM1 antibody or anti-Flk-1 antibody.

Supplementary Figure 4

Double immunofluorescence of *in situ* TUNEL (green) and anti-p75NTR antibody (red) in E12.5, E14.5 and E16.5 liver. (Original magnification; X200: upper panels, X400: lower panels)

References

1. Hautekeete ML, Geerts A. The hepatic stellate (Ito) cell: its role in human liver disease. Virchows Arch 1997;430:195-207.
2. Li Z, Dranoff JA, Chan EP, Uemura M, Sevigny J, Wells RG. Transforming growth factor-beta and substrate stiffness regulate portal fibroblast activation in culture. Hepatology 2007;46:1246-56.
3. Knittel T, Kobold D, Piscaglia F, Saile B, Neubauer K, Mehde M, Timpl R, Ramadori G. Localization of liver myofibroblasts and hepatic stellate cells in normal and diseased rat livers: distinct roles of (myo-)fibroblast subpopulations in hepatic tissue repair. Histochem Cell Biol 1999;112:387-401.
4. Taub R. Liver regeneration: from myth to mechanism. Nat Rev Mol Cell Biol 2004;5:836-47.
5. Friedman SL, Wei S, Blaner WS. Retinol release by activated rat hepatic lipocytes: regulation by Kupffer cell-conditioned medium and PDGF. Am J Physiol 1993;264:G947-52.
6. Tsukamoto H, Cheng S, Blaner WS. Effects of dietary polyunsaturated fat on ethanol-induced Ito cell activation. Am J Physiol 1996;270:G581-6.
7. Schmitt-Graff A, Kruger S, Bochard F, Gabbiani G, Denk H. Modulation of alpha smooth muscle actin and desmin expression in perisinusoidal cells of normal and diseased human livers. Am J Pathol 1991;138:1233-42.
8. Yamaoka K, Nouchi T, Marumo F, Sato C. Alpha-smooth-muscle actin expression in normal and fibrotic human livers. Dig Dis Sci 1993;38:1473-9.
9. Friedman SL. Molecular regulation of hepatic fibrosis, an integrated cellular response to tissue injury. J Biol Chem 2000;275:2247-50.
10. Kinnman N, Francoz C, Barbu V, Wendum D, Rey C, Hultcrantz R, Poupon R, Housset C. The myofibroblastic conversion of peribiliary fibrogenic cells distinct from hepatic stellate cells is stimulated by platelet-derived growth factor during liver fibrogenesis. Lab Invest 2003;83:163-73.
11. Guyot C, Lepreux S, Combe C, Doudnikoff E, Bioulac-Sage P, Balabaud C, Desmouliere A. Hepatic fibrosis and cirrhosis: the (myo)fibroblastic cell subpopulations involved. Int J Biochem Cell Biol 2006;38:135-51.
12. Burt AD, Robertson JL, Heir J, MacSween RN. Desmin-containing stellate cells in rat liver; distribution in normal animals and response to experimental acute liver injury. J Pathol 1986;150:29-35.
13. Neubauer K, Knittel T, Aurisch S, Fellmer P, Ramadori G. Glial fibrillary acidic protein--a cell type specific marker for Ito cells in vivo and in vitro. J Hepatol 1996;24:719-30.
14. Niki T, Pekny M, Hellemans K, Bleser PD, Berg KV, Vaeyens F, Quartier E, Schuit F, Geerts A. Class VI intermediate filament protein nestin is induced during activation of rat hepatic stellate cells. Hepatology 1999;29:520-7.
15. Knittel T, Aurisch S, Neubauer K, Eichhorst S, Ramadori G. Cell-type-specific expression of neural cell adhesion molecule (N-CAM) in Ito cells of rat liver. Up-regulation during in vitro activation and in hepatic tissue repair. Am J Pathol 1996;149:449-62.
16. Cassiman D, van Pelt J, De Vos R, Van Lommel F, Desmet V, Yap SH, Roskams T. Synaptophysin: A novel marker for human and rat hepatic stellate cells. Am J Pathol 1999;155:1831-9.
17. Cassiman D, Barlow A, Vander Borght S, Libbrecht L, Pachnis V. Hepatic stellate cells do not derive from

the neural crest. J Hepatol 2006;44:1098-104.

18. Baba S, Fujii H, Hirose T, Yasuchika K, Azuma H, Hoppo T, Naito M, Machimoto T, Ikai I. Commitment of bone marrow cells to hepatic stellate cells in mouse. J Hepatol 2004;40:255-60.

19. Geerts A. On the origin of stellate cells: mesodermal, endodermal or neuro-ectodermal? J Hepatol 2004;40:331-4.

20. Duncan SA. Mechanisms controlling early development of the liver. Mech Dev 2003;120:19-33.

21. Matsumoto K, Yoshitomi H, Rossant J, Zaret KS. Liver organogenesis promoted by endothelial cells prior to vascular function. Science 2001;294:559-63.

22. Knook DL, Seffelaar AM, de Leeuw AM. Fat-storing cells of the rat liver. Their isolation and purification. Exp Cell Res 1982;139:468-71.

23. Geerts A, Vrijsen R, Rauterberg J, Burt A, Schellinck P, Wisse E. In vitro differentiation of fat-storing cells parallels marked increase of collagen synthesis and secretion. J Hepatol 1989;9:59-68.

24. Blomhoff R, Berg T. Isolation and cultivation of rat liver stellate cells. Methods Enzymol 1990;190:58-71.

25. Greenwel P, Schwartz M, Rosas M, Peyrol S, Grimaud JA, Rojkind M. Characterization of fat-storing cell lines derived from normal and CCl4-cirrhotic livers. Differences in the production of interleukin-6. Lab Invest 1991;65:644-53.

26. Friedman SL, Rockey DC, McGuire RF, Maher JJ, Boyles JK, Yamasaki G. Isolated hepatic lipocytes and Kupffer cells from normal human liver: morphological and functional characteristics in primary culture. Hepatology 1992;15:234-43.

27. Bibel M, Barde YA. Neurotrophins: key regulators of cell fate and cell shape in the vertebrate nervous system. Genes Dev 2000;14:2919-37.

28. Campagnolo L, Russo MA, Puglianiello A, Favale A, Siracusa G. Mesenchymal cell precursors of peritubular smooth muscle cells of the mouse testis can be identified by the presence of the p75 neurotrophin receptor. Biol Reprod 2001;64:464-72.

29. Cassiman D, Denef C, Desmet VJ, Roskams T. Human and rat hepatic stellate cells express neurotrophins and neurotrophin receptors. Hepatology 2001;33:148-58.

30. Trim N, Morgan S, Evans M, Issa R, Fine D, Afford S, Wilkins B, Iredale J. Hepatic stellate cells express the low affinity nerve growth factor receptor p75 and undergo apoptosis in response to nerve growth factor stimulation. Am J Pathol 2000;156:1235-43.

31. Oakley F, Trim N, Constandinou CM, Ye W, Gray AM, Frantz G, Hillan K, Kendall T, Benyon RC, Mann DA, Iredale JP. Hepatocytes express nerve growth factor during liver injury: evidence for paracrine regulation of hepatic stellate cell apoptosis. Am J Pathol 2003;163:1849-58.

32. Asai K, Tamakawa S, Yamamoto M, Yoshie M, Tokusashi Y, Yaginuma Y, Kasai S, Ogawa K. Activated hepatic stellate cells overexpress p75NTR after partial hepatectomy and undergo apoptosis on nerve growth factor stimulation. Liver Int 2006;26:595-603.

33. Passino MA, Adams RA, Sikorski SL, Akassoglou K. Regulation of hepatic stellate cell differentiation by the neurotrophin receptor p75NTR. Science 2007;315:1853-6.

34. Geerts A. The simple truth is seldom true and never simple: dual role for p75(NTR) in transdifferentation and cell death of hepatic stellate cells. Hepatology 2007;46:600-1.

35. Tanimizu N, Nishikawa M, Saito H, Tsujimura T, Miyajima A. Isolation of hepatoblasts based on the expression of Dlk/Pref-1. J Cell Sci 2003;116:1775-86.

36. Nonaka H, Tanaka M, Suzuki K, Miyajima A. Development of murine hepatic sinusoidal endothelial cells characterized by the expression of hyaluronan receptors. Dev Dyn 2007;236:2258-67.

37. Lemaigre FP. Development of the biliary tract. Mech Dev 2003;120:81-7.

38. Li L, Krantz ID, Deng Y, Genin A, Banta AB, Collins CC, Qi M, Trask BJ, Kuo WL, Cochran J, Costa T, Pierpont ME, Rand EB, Piccoli DA, Hood L, Spinner NB. Alagille syndrome is caused by mutations in human Jagged1, which encodes a ligand for Notch1. Nat Genet 1997;16:243-51.

39. Oda T, Elkahloun AG, Pike BL, Okajima K, Krantz ID, Genin A, Piccoli DA, Meltzer PS, Spinner NB, Collins FS, Chandrasekharappa SC. Mutations in the human Jagged1 gene are responsible for Alagille syndrome. Nat